

Contents

1	Introduction	3
1.1	Definition, Notation and Classification	3
1.2	Finite difference method	5
1.3	von Neumann stability analysis	9
2	Advection Equation	13
2.1	FTCS Method	14
2.2	Upwind Methods	15
2.3	The Lax Method	18
2.4	The Lax-Wendroff method	22
3	Burgers Equation	27
3.1	Hopf-Cole Transformation	28
3.2	General Solution of the 1D Burgers Equation	29
3.3	Forced Burgers Equation	30
3.4	Numerical Treatment	31
4	The Wave Equation	35
4.1	The Wave Equation in 1D	35
4.1.1	Solution of the IVP	36
4.1.2	Numerical Treatment	37
4.1.3	Examples	40
4.2	The Wave Equation in 2D	44
4.2.1	Examples	44
5	Sine-Gordon Equation	45
5.1	Kink and antikink solitons	45
5.2	Numerical treatment	48
A	Tridiagonal matrix algorithm	53

B The Method of Characteristics..... 57
References 59

Chapter 1

Introduction

1.1 Definition, Notation and Classification

A differential equation involving more than one independent variable and its partial derivatives with respect to those variables is called a *partial differential equation* (PDE).

Consider a simple PDE of the form:

$$\frac{\partial}{\partial x}u(x,y) = 0.$$

This equation implies that the function $u(x,y)$ is independent of x . Hence the general solution of this equation is $u(x,y) = f(y)$, where f is an arbitrary function of y . The analogous ordinary differential equation is

$$\frac{du}{dx} = 0,$$

its general solution is $u(x) = c$, where c is a constant. This example illustrates that general solutions of ODEs involve arbitrary constants, whereas solutions of PDEs involve *arbitrary functions*.

In general, one can classify PDEs with respect to different criterion, e.g.:

- Order;
- Dimension;
- Linearity;
- Initial/Boundary value problem, etc.

By *order* of PDE we will understand the order of the highest derivative that occurs. A PDE is said to be *linear* if it is linear in unknown functions and their derivatives, with coefficients depending on the independent variables. The independent variables typically include one or more *space dimensions* and sometimes time dimension as well.

For example, the wave equation

$$\frac{\partial^2 u(x,t)}{\partial t^2} = a^2 \frac{\partial^2 u(x,t)}{\partial x^2}$$

is a one-dimensional, second-order linear PDE. In contrast, the Fisher Equation of the form

$$\frac{\partial u(\mathbf{r},t)}{\partial t} = \Delta u(\mathbf{r},t) + u(\mathbf{r},t) - u(\mathbf{r},t)^2,$$

where $\mathbf{r} = (x, y)$ is a two-dimensional, second-order nonlinear PDE.

Linear Second-Order PDEs

For linear PDEs in two dimensions there is a simple classification in terms of the general equation

$$au_{xx} + bu_{xy} + cu_{yy} + du_x + eu_y + fu + g = 0, \quad u = u(x, y),$$

where the coefficients a, b, c, d, e, f and g are real and in general can also be functions of x and y . The PDE's of this type are classified by the value of discriminant $D_\lambda = b^2 - 4ac$ of the eigenvalue problem for the matrix

$$A = \begin{pmatrix} a & b/2 \\ b/2 & c \end{pmatrix},$$

build from the coefficients of the highest derivatives. A simple classification is shown on the following table [20, 13]:

D_λ	Typ	Eigenvalues
$D_\lambda < 0$	<i>elliptic</i>	the same sign
$D_\lambda > 0$	<i>hyperbolic</i>	different signs
$D_\lambda = 0$	<i>parabolic</i>	zero is an eigenvalue

For instance, *the Laplace equation* for the electrostatic potential φ in the space without a charge

$$\frac{\partial^2 \varphi}{\partial x^2} + \frac{\partial^2 \varphi}{\partial y^2} = 0$$

is elliptic, as $a = c = 1, b = 0, D_\lambda = -4 < 0$. In general, elliptic PDEs describe processes that have already reached steady state, and hence are time-independent.

One-dimensional *wave equation* for some amplitude $A(x, t)$

$$\frac{\partial^2 A}{\partial t^2} - v^2 \frac{\partial^2 A}{\partial x^2} = 0$$

with the positive dispersion velocity v is hyperbolic ($a = 1, b = 0, c = -v^2, D_\lambda = 4v^2 > 0$). Hyperbolic PDEs describe time-dependent, conservative processes, such as convection, that are not evolving toward steady state.

The next example is a *diffusion equation* for the particle's density $\rho(x, t)$

$$\frac{\partial \rho}{\partial t} = D \frac{\partial^2 \rho}{\partial x^2},$$

where $D > 0$ is a diffusion coefficient. This equation is called to be parabolic ($a = -D, b = c = 0, D_\lambda = 0$). Parabolic PDEs describe time-dependent, dissipative processes, such as diffusion, that are evolving toward steady state.

Each of these classes should be investigated separately as different methods are required for each class. The next point to emphasize is that as all the coefficients of the PDE can depend on x and y , this classification concept is *local*.

Initial and Boundary-Value Problems

As it was mentioned above the solution of PDEs involve arbitrary functions. That is, in order to solve the system in question completely, additional conditions are needed. These conditions can be given in the form of *initial* and *boundary* conditions. Initial conditions define the values of the dependent variables at the initial stage (e.g. at $t = 0$), whereas the boundary conditions give the information about the value of the dependent variable or its derivative on the boundary of the area of interest. Typically, one distinguishes

- *Dirichlet conditions* specify the values of the dependent variables of the boundary points.
- *Neumann conditions* specify the values of the normal gradients of the boundary.
- *Robin conditions* defines a linear combination of the Dirichlet and Neumann conditions.

Moreover, it is useful to classify the PDE in question in terms of *initial value problem (IVP)* and *boundary value problem (BVP)*.

- *Initial value problem*: PDE in question describes *time evolution*, i.e., the initial space-distribution is given; the goal is to find how the dependent variable propagates in time (e.g., the diffusion equation).
- *Boundary value problem*: A static solution of the problem should be found in some region-and the dependent variable is specified on its boundary (e.g., the Laplace equation).

1.2 Finite difference method

Let us consider a one-dimensional PDE for the unknown function $u(x, t)$. One way to numerically solve the PDE is to approximate all the derivatives by *finite differences*. We divide the domain in space using a *mesh* x_0, x_1, \dots, x_N and in time using a mesh t_0, t_1, \dots, t_T . First we assume a *uniform partition* both in space and in time, so that the difference between two consecutive space points will be Δx and between two consecutive time points will be Δt , i.e.,

$$\begin{aligned}x_i &= x_0 + i\Delta x, & i &= 0, 1, \dots, M; \\t_j &= t_0 + j\Delta t, & j &= 0, 1, \dots, T;\end{aligned}$$

The Taylor series method

Consider a Taylor expansion of an analytical function $u(x)$.

$$u(x + \Delta x) = u(x) + \sum_{n=1}^{\infty} \frac{\Delta x^n}{n!} \frac{\partial^n u}{\partial x^n} = u(x) + \Delta x \frac{\partial u}{\partial x} + \frac{\Delta x^2}{2!} \frac{\partial^2 u}{\partial x^2} + \frac{\Delta x^3}{3!} \frac{\partial^3 u}{\partial x^3} + \dots \quad (1.1)$$

Then for the first derivative one obtains:

$$\frac{\partial u}{\partial x} = \frac{u(x + \Delta x) - u(x)}{\Delta x} - \frac{\Delta x}{2!} \frac{\partial^2 u}{\partial x^2} + \frac{\Delta x^2}{3!} \frac{\partial^3 u}{\partial x^3} - \dots \quad (1.2)$$

If we break the right hand side of the last equation after the first term, for $\Delta x \ll 1$ the last equation becomes

$$\boxed{\frac{\partial u}{\partial x} = \frac{u(x + \Delta x) - u(x)}{\Delta x} + \mathcal{O}(\Delta x) = \frac{\Delta_i u}{\Delta x} + \mathcal{O}(\Delta x)}, \quad (1.3)$$

where

$$\Delta_i u = u(x + \Delta x) - u(x) := u_{i+1} - u_i$$

is called a *forward difference*. The backward expansion of the function u can be written as $\Delta x \ll 1$ the last equation reads

$$u(x + (-\Delta x)) = u(x) - \Delta x \frac{\partial u}{\partial x} + \frac{\Delta x^2}{2!} \frac{\partial^2 u}{\partial x^2} - \frac{\Delta x^3}{3!} \frac{\partial^3 u}{\partial x^3} + \dots, \quad (1.4)$$

so for the first derivative one obtains

$$\boxed{\frac{\partial u}{\partial x} = \frac{u(x) - u(x - \Delta x)}{\Delta x} + \mathcal{O}(\Delta x) = \frac{\nabla_i u}{\Delta x} + \mathcal{O}(\Delta x)}, \quad (1.5)$$

where

$$\nabla_i u = u(x) - u(x - \Delta x) := u_i - u_{i-1}$$

is called a *backward difference*. One can see that both forward and backward differences are of the order $\mathcal{O}(\Delta x)$. We can combine these two approaches and derive a *central difference*, which yields a more accurate approximation. If we subtract Eq. (1.5) from Eq. (1.3) one obtains

$$u(x + \Delta x) - u(x - \Delta x) = 2\Delta x \frac{\partial u}{\partial x} + 2\frac{\Delta x^3}{3!} \frac{\partial^3 u}{\partial x^3} + \dots, \quad (1.6)$$

what is equivalent to

$$\boxed{\frac{\partial u}{\partial x} = \frac{u(x + \Delta x) - u(x - \Delta x)}{2\Delta x} + \mathcal{O}(\Delta x^2)}$$
 (1.7)

Note that the central difference (1.7) is of the order of $\mathcal{O}(\Delta^2 x)$.

The second derivative can be found in the same way using the linear combination of different Taylor expansions. For instance, consider

$$u(x + 2\Delta x) = u(x) + 2\Delta x \frac{\partial u}{\partial x} + \frac{(2\Delta x)^2}{2!} \frac{\partial^2 u}{\partial x^2} + \frac{(2\Delta x)^3}{3!} \frac{\partial^3 u}{\partial x^3} + \dots$$
 (1.8)

Subtracting from the last equation Eq. (1.1), multiplied by two, one gets the following equation

$$u(x + 2\Delta x) - 2u(x + \Delta x) = -u(x) + \Delta x^2 \frac{\partial^2 u}{\partial x^2} + \Delta x^3 \frac{\partial^3 u}{\partial x^3} + \dots$$
 (1.9)

Hence one can approximate the second derivative as

$$\boxed{\frac{\partial^2 u}{\partial x^2} = \frac{u(x + 2\Delta x) - 2u(x + \Delta x) + u(x)}{\Delta x^2} + \mathcal{O}(\Delta x)}$$
 (1.10)

Similarly one can obtain the expression for the second derivative in terms of backward expansion, i.e.,

$$\boxed{\frac{\partial^2 u}{\partial x^2} = \frac{u(x - 2\Delta x) - 2u(x - \Delta x) + u(x)}{\Delta x^2} + \mathcal{O}(\Delta x)}$$
 (1.11)

Finally, if we add Eqn. (1.3) and (1.5) an expression for the central second derivative reads

$$\boxed{\frac{\partial^2 u}{\partial x^2} = \frac{u(x + \Delta x) - 2u(x) + u(x - \Delta x)}{\Delta x^2} + \mathcal{O}(\Delta x^2)}$$
 (1.12)

One can see that approximation (1.12) provides more accurate approximation as (1.10) and (1.11).

In an analogous way one can obtain finite difference approximations to higher order derivatives and differential operators. The coefficients for first three derivatives for the case of forward, backward and central differences are given in Tables 1.1, 1.2, 1.3.

Mixed derivatives

A finite difference approximations for the mixed partial derivatives can be calculated in the same way. For example, let us find the central approximation for the derivative

	u_i	u_{i+1}	u_{i+2}	u_{i+3}	u_{i+4}
$\Delta x \frac{\partial u}{\partial x}$	-1	1			
$\Delta x^2 \frac{\partial^2 u}{\partial x^2}$	1	-2	1		
$\Delta x^3 \frac{\partial^3 u}{\partial x^3}$	-1	3	-3	1	
$\Delta x^4 \frac{\partial^4 u}{\partial x^4}$	1	-4	6	-4	1

Table 1.1 Forward difference quotient, $\mathcal{O}(\Delta x)$

	u_{i-4}	u_{i-3}	u_{i-2}	u_{i-1}	u_i
$\Delta x \frac{\partial u}{\partial x}$				-1	1
$\Delta x^2 \frac{\partial^2 u}{\partial x^2}$			1	-2	1
$\Delta x^3 \frac{\partial^3 u}{\partial x^3}$		-1	3	-3	1
$\Delta x^4 \frac{\partial^4 u}{\partial x^4}$	1	-4	6	-4	1

Table 1.2 Backward difference quotient, $\mathcal{O}(\Delta x)$

	u_{i-2}	u_{i-1}	u_i	u_{i+1}	u_{i+2}
$2\Delta x \frac{\partial u}{\partial x}$		-1	0	1	
$\Delta x^2 \frac{\partial^2 u}{\partial x^2}$		1	-2	1	
$2\Delta x^3 \frac{\partial^3 u}{\partial x^3}$	-1	2	0	-2	1
$\Delta x^4 \frac{\partial^4 u}{\partial x^4}$	1	-4	6	-4	1

Table 1.3 Central difference quotient, $\mathcal{O}(\Delta x^2)$

$$\begin{aligned} \frac{\partial^2 u}{\partial x \partial y} &= \frac{\partial}{\partial x} \left(\frac{\partial u}{\partial y} \right) = \frac{\partial}{\partial x} \left(\frac{u(x, y + \Delta y) - u(x, y - \Delta y)}{2\Delta y} + \mathcal{O}(\Delta y^2) \right) = \\ &= \frac{u(x + \Delta x, y + \Delta y) - u(x - \Delta x, y + \Delta y) - u(x + \Delta x, y - \Delta y) + u(x - \Delta x, y - \Delta y)}{4\Delta x \Delta y} + \mathcal{O}(\Delta x^2 \Delta y^2). \end{aligned}$$

A nonequidistant mesh

In the section above we have considered different numerical approximations for the derivatives using the equidistant mesh. However, in many applications it is convenient to use a nonequidistant mesh, where the spatial steps fulfill the following rule:

$$\Delta x_i = \alpha \Delta x_{i-1}.$$

If $\alpha = 1$ the mesh is said to be equidistant. Let us now calculate the first derivative of the function $u(x)$ of the second-order accuracy:

$$u(x + \alpha \Delta x) = u(x) + \alpha \Delta x \frac{\partial u}{\partial x} + \frac{(\alpha \Delta x)^2}{2!} \frac{\partial^2 u}{\partial x^2} + \frac{(\alpha \Delta x)^3}{3!} \frac{\partial^3 u}{\partial x^3} + \dots \quad (1.13)$$

Adding the last equation with Eq. (1.4) multiplied by α one obtains the expression for the second derivative

$$\frac{\partial^2 u}{\partial x^2} = \frac{u(x + \alpha \Delta x) - (1 + \alpha)u(x) + \alpha u(x - \Delta x)}{\frac{1}{2}\alpha(\alpha + 1)\Delta x^2} + \mathcal{O}(\Delta x) \quad (1.14)$$

Substitution of the last equation into Eq. (1.4) yields

$$\boxed{\frac{\partial u}{\partial x} = \frac{u(x + \alpha \Delta x) - (1 - \alpha^2)u(x) - \alpha^2 u(x - \Delta x)}{\alpha(\alpha + 1)\Delta x} + \mathcal{O}(\Delta x^2)}. \quad (1.15)$$

1.3 von Neumann stability analysis

One of the central questions arising by numerical treatment of the problem in question is stability of the numerical scheme we are interested in [15]. An algorithm for solving an evolutionary partial differential equation is said to be *stable*, if the numerical solution at a fixed time remains bounded as the step size goes to zero, so the perturbations in form of, e.g., rounding error does not increase in time. Unfortunately, there are no general methods to verify the numerical stability for the partial differential equations in general form, so one restrict oneself to the case of linear PDE's. The standard method for linear PDE's with periodic boundary conditions was proposed by John von Neumann [6, 2] and is based on the representation of the rounding error in form of the Fourier series.

In order to illustrate the procedure, let us introduce the following notation:

$$u^{j+1} = \mathcal{T}[u^j]. \quad (1.16)$$

Here \mathcal{T} is a nonlinear operator, depending on the numerical scheme in question. The successive application of \mathcal{T} results in a sequence of values

$$u^0, u^1, u^2, \dots,$$

that approximate the exact solution of the problem. However, at each time step we add a small error ε^j , i.e., the sequence above reads

$$u^0 + \varepsilon^0, u^1 + \varepsilon^1, u^2 + \varepsilon^2, \dots,$$

where ε^j is a cumulative rounding error at time t_j . Thus we obtain

$$u^{j+1} + \varepsilon^{j+1} = \mathcal{T}(u^j + \varepsilon^j). \quad (1.17)$$

After linearization of the last equation (we suppose that Taylor expansion of \mathcal{T} is possible) the linear equation for the perturbation takes the form:

$$\boxed{\varepsilon^{j+1} = \frac{\partial \mathcal{T}(u^j)}{\partial u^j} \varepsilon^j := G \varepsilon^j}. \quad (1.18)$$

This equation is called *the error propagation law*, whereas the linearization matrix G is said to be *an amplification matrix* [10]. Now, the stability of the numerical scheme in question depends on the eigenvalues g_μ of the matrix G . In other words, the scheme is stable if and only if

$$|g_\mu| \leq 1 \quad \forall \mu$$

Now the question is how this information can be used in practice. The first point to emphasize is that in general one deals with the $u(x_i, t_j) := u_i^j$, so one can write

$$\varepsilon_i^{j+1} = \sum_{i'} G_{ii'} \varepsilon_{i'}^j, \quad (1.19)$$

where

$$G_{ii'} = \frac{\partial \mathcal{T}(u^j)_i}{\partial u_{i'}^j}.$$

Furthermore, the spatial variation of ε_i^j (rounding error at the time step t_j at the point x_i) can be expanded in a finite Fourier series in the interval $[0, L]$:

$$\varepsilon_i^j = \sum_k e^{ikx_i} \tilde{\varepsilon}^j(k), \quad (1.20)$$

where k is the wavenumber and $\tilde{\varepsilon}^j(k)$ are the Fourier coefficients. Since the rounding error tends to grow or decay exponentially with time, it is reasonable to assume that $\tilde{\varepsilon}^j(k)$ varies exponentially with time, i.e.,

$$\varepsilon_i^j = \sum_k e^{\omega t_j} e^{ikx_i},$$

where ω is a constant. The next point to emphasize is that the functions e^{ikx_i} are eigenfunctions of the matrix G , so the last expansion can be interpreted as the expansion in eigenfunctions of G . In addition, the equation for the error is linear, so it is enough to examine the growth of the error of a typical term of the sum. Thus, from the practical point of view one takes the error ε_i^j just as

$$\varepsilon_i^j = e^{\omega t_j} e^{ikx_i}.$$

The substitution of this expression into Eq. (1.20) results in the following relation

$$\varepsilon_i^{j+1} = g(k) \varepsilon_i^j. \quad (1.21)$$

That is, one can interpret e^{ikx_i} as an eigenvector corresponding to the eigenvalue $g(k)$. The value $g(k)$ is often called *an amplification factor*. Finally, the stability criterion is then given by

$$\boxed{|g(k)| \leq 1 \quad \forall k}. \quad (1.22)$$

This criterion is called *von Neumann stability criterion*.

Notice that presented stability analysis can be applied only in certain cases. Namely, the linear PDE in question should be with constant coefficients and satisfies periodic boundary conditions. In addition, the corresponding difference scheme should possess no more than two time levels [19]. However, it is often used in more complicated situations as a good estimation for the step sizes used in the approximation.

Chapter 2

Advection Equation

Let us consider a continuity equation for the one-dimensional drift of incompressible fluid. In the case that a particle density $u(x, t)$ changes only due to convection processes one can write

$$u(x, t + \Delta t) = u(x - c \Delta t, t).$$

If Δt is sufficient small, the Taylor-expansion of both sides gives

$$u(x, t) + \Delta t \frac{\partial u(x, t)}{\partial t} \simeq u(x, t) - c \Delta t \frac{\partial u(x, t)}{\partial x}$$

or, equivalently

$$\frac{\partial u}{\partial t} + c \frac{\partial u}{\partial x} = 0. \quad (2.1)$$

Here $u = u(x, t)$, $x \in \mathbb{R}$, and c is a nonzero constant velocity. Equation (2.1) is called to be *an advection equation* and describes the motion of a scalar u as it is advected by a known velocity field. According to the classification given in Sec. 1.1, Eq. (2.1) is a hyperbolic PDE. The unique solution of (2.1) is determined by an initial condition $u_0 := u(x, 0)$

$$u(x, t) = u_0(x - ct), \quad (2.2)$$

where $u_0 = u_0(x)$ is an arbitrary function defined on \mathbb{R} .

One way to find this exact solution is the method of characteristics (see App. B). In the case of Eq. (2.1) the coefficients $A = c$, $B = 1$, $C = 0$ and Eqn. (B.2) read

$$\begin{aligned} \frac{dt}{ds} = 1 &\Leftrightarrow |t(0) = 0| \Leftrightarrow t = s, \\ \frac{dx}{ds} = c &\Leftrightarrow |x(0) = x_0| \Leftrightarrow x = x_0 + ct. \end{aligned}$$

That is, for the advection equation (2.1) characteristic curves are represented by straight lines (see Fig. 2.1). Hence, Eq. (B.3) becomes

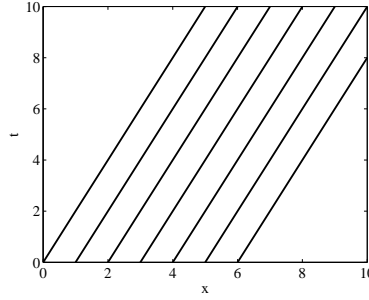


Fig. 2.1 Characteristic curves $x = x_0 + ct$, $s = t$ for advection equation (2.1) are shown for different values of c .

$$\frac{du}{ds} = 0 \quad \text{with} \quad u(0) = u_0(x_0).$$

Alltogether the solution of (2.1) takes the form (2.2). The solution (2.2) is just an initial function u_0 shifted by ct to the right (for $c > 0$) or to the left ($c < 0$), which remains constant along the characteristic curves ($du/ds = 0$).

2.1 FTCS Method

Now we focus on different explicit methods to solve advection equation (2.1) numerically on the periodic domain $[0, L]$ with a given initial condition $u_0 = u(x, 0)$.

We start the discussion of Eq. (2.1) with a so-called FTCS (forward in time, centered in space) method. As discussed in Sec. 1.2 we introduce the discretization in time on the uniform grid

$$t_j = t_0 + j \Delta t, \quad j = 0 \dots T.$$

Furthermore, in the x -direction, we use the uniform grid in the same manner

$$x_i = a + i \Delta x, \quad i = 0 \dots M, \quad \Delta x = \frac{L}{M}.$$

Adopting a forward temporal difference scheme (1.3), and a centered spatial difference scheme (1.7), Eq. (2.1) yields

$$\begin{aligned} \frac{u_i^{j+1} - u_i^j}{\Delta t} &= -c \frac{u_{i+1}^j - u_{i-1}^j}{2\Delta x} \Leftrightarrow \\ u_i^{j+1} &= u_i^j - \frac{c\Delta t}{2\Delta x} \left(u_{i+1}^j - u_{i-1}^j \right). \end{aligned} \quad (2.3)$$

Here we use a notation $u_i^j := u(x_i, t_j)$. Schematic representation of the FTCS approximation (2.3) is shown on Fig. 2.2.

von Neumann Stability Analysis

To investigate stability of the scheme (2.3) we follow the concept of von Neumann, introduced in Sec. 1.3. The usual ansatz

$$\varepsilon_i^j \sim e^{ikx_i}$$

leads to the following relation

$$\varepsilon_i^{j+1} = e^{ikx_i} - \frac{c\Delta t}{2\Delta x} \left(e^{ik(x_i+\Delta x)} - e^{ik(x_i-\Delta x)} \right) = \underbrace{\left(1 - \frac{c\Delta t}{2\Delta x} \left(e^{ik\Delta x} - e^{-ik\Delta x} \right) \right)}_{g(k)} \varepsilon_i^j,$$

where ε_i^{j+1} stands for the cumulative rounding error at time t_j . The von Neumann's stability condition (1.22) for the amplification factor $g(k)$ reads:

$$|g(k)| \leq 1 \quad \forall k.$$

In our case one obtains:

$$|g(k)|^2 = 1 + \frac{c^2\Delta t^2}{\Delta x^2} \sin^2(k\Delta x),$$

One can see that the magnitude of the amplification factor $g(k)$ is greater than unity for all k . This implies that the instability occurs for all given c , Δt and Δx , i.e., the FTCS scheme (2.3) is *unconditionally unstable*.

2.2 Upwind Methods

The next simple scheme we are interested in belongs to the class of so-called *upwind methods* – numerical discretization schemes for solving hyperbolic PDEs. The idea of this method is that the spatial differences are skewed in the “upwind” direction, i.e., the direction from which the advecting flow originates. The origin of upwind methods can be traced back to the work of R. Courant et al. [5].

The simplest upwind schemes possible are given by

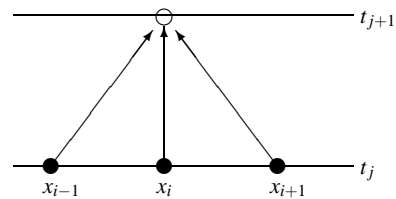


Fig. 2.2 Schematic visualization of the FTCS-method (2.3).

$$\begin{aligned} \frac{u_i^{j+1} - u_i^j}{\Delta t} &= -c \frac{u_i^j - u_{i-1}^j}{\Delta x} \Leftrightarrow \\ u_i^{j+1} &= u_i^j - \frac{c\Delta t}{\Delta x} (u_i^j - u_{i-1}^j), \quad (c > 0). \end{aligned} \quad (2.4)$$

and

$$\begin{aligned} \frac{u_i^{j+1} - u_i^j}{\Delta t} &= -c \frac{u_{i+1}^j - u_i^j}{\Delta x} \Leftrightarrow \\ u_i^{j+1} &= u_i^j - \frac{c\Delta t}{\Delta x} (u_{i+1}^j - u_i^j) \quad (c < 0). \end{aligned} \quad (2.5)$$

Note that the upwind scheme (2.4) corresponds to the case of positive velocities c , whereas Eq. (2.5) stands for the case $c < 0$. The next point to emphasize is that both schemes (2.4)–(2.5) are only first-order in space and time. Schematic representations of both upwind methods is presented on Fig. 2.3

In the matrix form the upwind scheme (2.4) takes the form

$$\mathbf{u}^{j+1} = A\mathbf{u}^j, \quad (2.6)$$

where \mathbf{u}^j is a vector on the time step j and A is a $n \times n$ matrix ($h := \Delta t / \Delta x$),

$$A = \begin{pmatrix} 1 - ch & 0 & 0 & \dots & \boxed{ch} \\ ch & 1 - ch & 0 & \dots & 0 \\ 0 & ch & 1 - ch & \dots & 0 \\ \dots & \dots & \dots & \dots & \dots \\ 0 & \dots & ch & 1 - ch & \dots \end{pmatrix}$$

The boxed element A_{1n} indicates the influence of the periodic boundary conditions. Similarly, one can also represent the scheme (2.5) in the form (2.6) with matrix

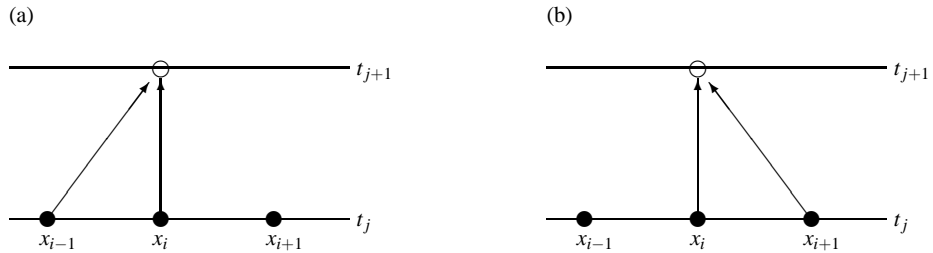


Fig. 2.3 Schematic visualization of the first-order upwind methods. (a) Upwind scheme (2.4) for $c > 0$. (b) Upwind scheme (2.5) for $c < 0$.

$$A = \begin{pmatrix} 1+ch & -ch & 0 & \dots & 0 \\ 0 & 1+ch & -ch & \dots & 0 \\ \dots & \dots & \dots & \dots & \dots \\ 0 & \dots & 1+ch & -ch & \\ \boxed{-ch} & \dots & 0 & 1+ch & \end{pmatrix}$$

Again, the boxed element A_{n1} displays the influence of periodic boundary conditions.

von Neumann Stability Analysis

In order to investigate the stability of the upwind scheme (2.4) (or (2.5)) we start with the usual ansatz

$$\varepsilon_i^j \sim e^{ikx_i},$$

leading to the equation for the cumulative rounding error at time t_{j+1}

$$\varepsilon_i^{j+1} = g(k)\varepsilon_i^j,$$

where the amplification factor $g(k)$ for, e.g., the upwind scheme (2.4) is given by

$$g(k) = 1 - \frac{c\Delta t}{\Delta x} \left(1 - e^{-ik\Delta x} \right) = \left| \alpha = \frac{c\Delta t}{\Delta x}, \varphi = -k\Delta x \right| = 1 - \alpha + \alpha e^{i\varphi}.$$

The stability condition (1.22) is fulfilled for all k as long as

$$|g(k)| \leq 1 \Leftrightarrow 1 - \alpha \leq 0 \Leftrightarrow \boxed{\frac{c\Delta t}{\Delta x} \leq 1 \Leftrightarrow c \leq \frac{\Delta x}{\Delta t}}. \quad (2.7)$$

That is, the method (2.4) is *conditionally stable*, i.e., is stable if and only if the "physical" velocity c is not bigger than the spreading velocity $\Delta x/\Delta t$ of the numerical method. This is equivalent to the condition that the time step, Δt , must be smaller than the time taken for the wave to travel the distance of the spatial step, Δx . Schematic illustration of stability condition (2.7) is shown on Fig. . Condition (2.7) is called a *Courant-Friedrichs-Lewy (CFL)* stability criterion, whereas α is called a *Courant number*. The condition (2.7) is named after R. Courant, K. Friedrichs, and H. Lewy, who described it in their paper in 1928 [16].

Numerical results

Figure 2.5 shows an example of the calculation in which the upwind scheme (2.4) is used to advect a Gaussian pulse. Parameters of the calculation are chosen as

Fig. 2.4 Advection of a one-dimensional Gaussian shaped pulse $u_0 = \exp(-(x - 0.2)^2)$ with the scheme (2.4). Numerical calculation performed on the interval $x \in [0, 10]$ using $c = 0.5$, $\Delta t = 0.05$, $\Delta x = 0.1$. Numerical solutions at different times $t = 0$, $t = 50$, $t = 100$, $t = 150$, $t = 200$ are shown.

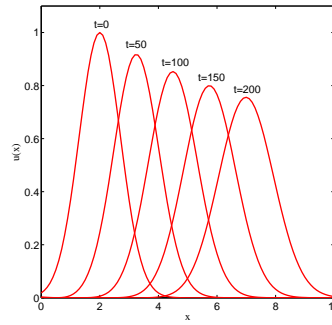
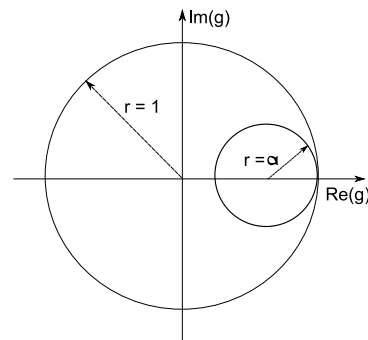


Fig. 2.5 Schematic illustration of the stability condition (2.7) for the upwind-method (2.4).



Space interval	$L=10$
Initial condition	$u_0(x) = \exp(-(x-2)^2)$
Space discretization step	$\Delta x = 0.1$
Time discretization step	$\Delta t = 0.05$
Velocity	$c = 0.5$
Amount of time steps	$T = 200$

For parameter values given above the stability condition (2.7) is fulfilled, so the scheme (2.4) is stable. On the other hand, one can see, that the wave-form shows evidence of dispersion. We discuss this problem in details in the next section.

2.3 The Lax Method

Let us consider a minor modification of the FTCS-method (2.3), in which the term u_i^j has been replaced by an average over its two neighbours (see Fig. 2.6):

$$u_i^{j+1} = \frac{1}{2} \left(u_{i+1}^j + u_{i-1}^j \right) - \frac{c\Delta t}{2\Delta x} \left(u_{i+1}^j - u_{i-1}^j \right). \quad (2.8)$$

In this case the matrix A of the linear system (2.6) is given by a sparse matrix with zero main diagonal

$$A = \begin{pmatrix} 0 & a & 0 & 0 & \dots & 0 & 0 & \boxed{b} \\ b & 0 & a & 0 & \dots & 0 & 0 & 0 \\ 0 & b & 0 & a & \dots & 0 & 0 & 0 \\ \dots & \dots \\ \dots & \dots \\ 0 & 0 & 0 & 0 & \dots & b & 0 & a \\ \boxed{a} & 0 & 0 & 0 & \dots & 0 & b & 0 \end{pmatrix},$$

where

$$a = \frac{1}{2} - \frac{c\Delta t}{2\Delta x},$$

$$b = \frac{1}{2} + \frac{c\Delta t}{2\Delta x}.$$

and the boxed elements represent the influence of periodic boundary conditions.

von Neumann stability analysis

In the case of the scheme (2.8) the amplification factor $g(k)$ becomes

$$g(k) = \cos k\Delta x - i \frac{c\Delta t}{\Delta x} \sin k\Delta x.$$

With $\alpha = \frac{c\Delta t}{\Delta x}$ and $\varphi(k) = k\Delta x$ one obtains

$$|g(k)|^2 = \cos^2 \varphi(k) + \alpha^2 \sin^2 \varphi(k) = 1 - (1 - \alpha^2) \sin^2 \varphi(k).$$

The stability condition (1.22) is fulfilled for all k as long as

$$1 - \alpha^2 \geq 0 \Leftrightarrow \frac{c\Delta t}{\Delta x} \leq 1,$$

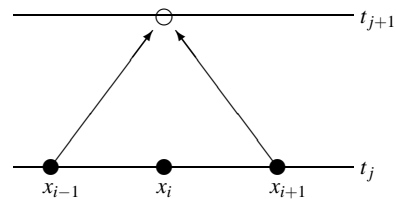


Fig. 2.6 Schematic visualization of the Lax method (2.8).

which is again the Courant-Friedrichs-Lewy condition (2.7). In fact, all stable *explicit* differencing schemes for solving the advection equation (2.1) are subject to the CFL constraint, which determines the maximum allowable time-step Δt .

Numerical results

Consider a realization of the Lax method (2.8) on the concrete numerical example:

Space interval	$L=10$
Initial condition	$u_0(x) = \exp(-10(x-2)^2)$
Space discretization step	$\Delta x = 0.05$
Time discretization step	$\Delta t = 0.05$
Velocity	$c = 0.5$
Amount of time steps	$T = 200$

As can be seen from Fig. 2.7 (a) like the upwind method (2.4), the Lax scheme introduces a spurious *dispersion* effect into the advection problem (2.1). Although the pulse is advected at the correct speed (i.e., it appears approximately stationary in the co-moving frame $x - ct$ (see Fig. 2.7 (b))), it does not remain the same shape as it should.

Fourier Analysis

One can try to understand the origin of the dispersion effect with the help of the dispersion relation. The ansatz of the Fourier mode of the form

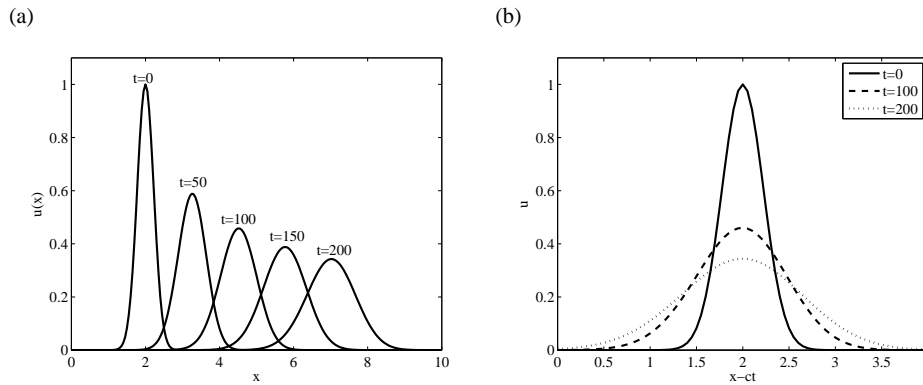


Fig. 2.7 Numerical implementation of the Lax method (2.8). Parameters: Advection velocity is $c = 0.5$, length of the space interval is $L = 10$, space and time discretization steps are $\Delta x = 0.05$ and $\Delta t = 0.05$, amount of time steps is $T = 200$, and initial condition is $u_0(x) = \exp(-10(x-2)^2)$. (a) Time evolution of $u(x, t)$ for different time moments. Solutions at $t = 0, 100, 150, 200$ are shown. (b) Time evolution in the co-moving frame $x - ct$ at $t = 0, 100, 200$.

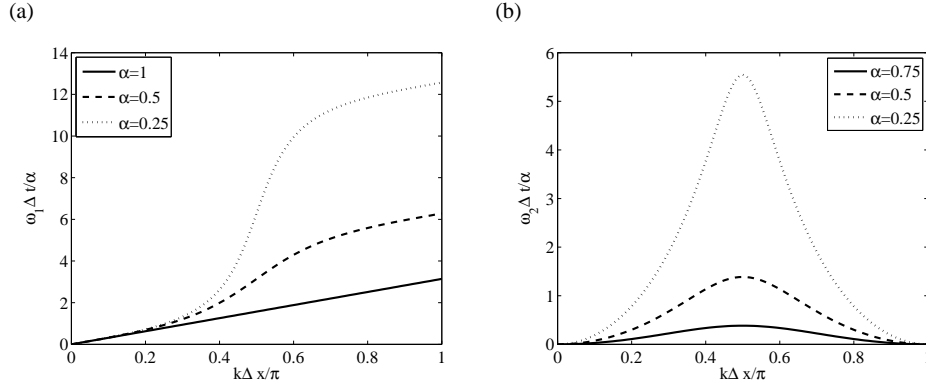


Fig. 2.8 Illustration of the dispersion relation for the Lax method calculated for different values of the Courant number α . (a) Real part of ω . (b) Imaginary part of ω .

$$u_i^j \sim e^{ikx_i - i\omega t_j}$$

for Eq. (2.8) results in the following relation

$$e^{-i\omega\Delta t} = \cos k\Delta x - i\alpha \sin k\Delta x,$$

where again $\alpha = c\Delta t / \Delta x$. For $\alpha = 1$ the right hand side of this relation is equal to $\exp(-ik\Delta x)$ and one obtains

$$\omega = k \frac{\Delta x}{\Delta t} = k \cdot c.$$

That is, in this case the Lax method (2.8) is exact (the phase velocity ω/k is equal c). However, in general case one should suppose $\omega = \omega_1 - i\omega_2$, i.e., the Fourier modes are of the form

$$u(x, t) \sim e^{ikx - i(\omega_1 - i\omega_2)t} = e^{i(kx - \omega_1 t)} e^{-\omega_2 t}$$

and the corresponding dispersion relation reads

$$\omega \Delta t = (\omega_1 - i\omega_2) \Delta t = i \ln(\cos k\Delta x - i\alpha \sin k\Delta x). \quad (2.9)$$

Hence, if $\omega_2 \geq 0$ one has deal with damped waves, that decay exponentially with the time constant $1/\omega_2$. Furthermore, from Eq. (2.9) can be seen, that for $\alpha < 1$ Fourier modes with wavelength about some grid constants ($\lambda = 2\pi/k \approx 4\Delta x$) are not only damped (see Fig 2.8 (b)) but, on the other hand, propagate with the essential greater phase velocity ω_1/k as long-wave components (see Fig. 2.8 (a)). Now the question we are interested in is what is the reason for this unphysical behavior? To answer this question let us rewrite the differential scheme (2.8):

$$\underbrace{\frac{1}{2}u_i^{j+1} + \frac{1}{2}u_i^{j+1}}_{u_i^{j+1}} - \underbrace{\frac{1}{2}u_i^{j-1} + \frac{1}{2}u_i^{j-1}}_0 = \frac{1}{2}(u_{i+1}^j + u_{i-1}^j) + \underbrace{u_i^j - u_i^j}_0 - \frac{c\Delta t}{2\Delta x}(u_{i+1}^j - u_{i-1}^j) \Leftrightarrow$$

$$\frac{1}{2}(u_i^{j+1} - u_i^{j-1}) = \frac{1}{2}(u_{i+1}^j - 2u_i^j + u_{i-1}^j) - \frac{c\Delta t}{2\Delta x}(u_{i+1}^j - u_{i-1}^j) - \frac{1}{2}(u_i^{j+1} - 2u_i^j + u_i^{j-1}),$$

or, in the continuous limit,

$$\frac{\partial u}{\partial t} = \frac{\Delta x^2}{2\Delta t} \frac{\partial^2 u}{\partial x^2} - c \frac{\partial u}{\partial x} - \frac{\Delta t^2}{2} \frac{\partial^2 u}{\partial t^2} \quad (2.10)$$

Although the last term in (2.10) tends to zero as $\Delta t \rightarrow 0$, the behavior of the first term depends on the behavior of Δt and Δx . That is, the Lax method is not a consistent way to solve Eq. (2.1). This message becomes clear if one calculates the partial derivative

$$\frac{\partial^2 u}{\partial t^2} \stackrel{(2.1)}{=} c^2 \frac{\partial^2 u}{\partial x^2}.$$

Substitution of the last expression into Eq. (2.10) results in the equation, which in addition to the advection term includes diffusion term as well,

$$\frac{\partial u}{\partial t} = -c \frac{\partial u}{\partial x} + D \frac{\partial^2 u}{\partial x^2},$$

where

$$D = \frac{\Delta x^2}{2\Delta t} - c^2 \frac{\Delta t}{2}$$

is a positive diffusion constant. Now the unphysical behavior of the Fourier modes becomes clear—we have integrated *the wrong equation!* That is, other numerical approximations should be used to solve Eq. (2.1) in a more correct way.

2.4 The Lax-Wendroff method

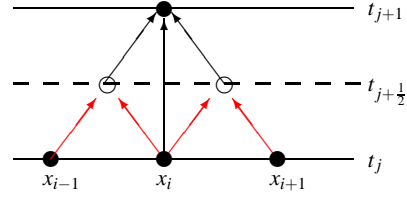
The Lax-Wendroff method, named after P. Lax and B. Wendroff [12], can be derived in a variety of ways. Let us consider two of them. The first way is based on the idea of so-called *multistep* methods. First of all let us calculate u_i^{j+1} using the information on the half time step:

$$u_i^{j+\frac{1}{2}} = u_i^j + \frac{\Delta t}{2} \left(-c \frac{\partial u}{\partial x} \Big|_{(i,j)} \right),$$

$$u_i^{j+1} = u_i^j + \Delta t \left(-c \frac{\partial u}{\partial x} \Big|_{(i,j+\frac{1}{2})} \right).$$

Now we use the central difference to approximate the derivative $u_x|_{i,j+\frac{1}{2}}$, i.e.,

Fig. 2.9 Schematical visualization of the Lax-Wendroff method (2.11).



$$u_i^{j+1} = u_i^j - \frac{c\Delta t}{\Delta x} \left(u_{i+\frac{1}{2}}^{j+\frac{1}{2}} - u_{i-\frac{1}{2}}^{j+\frac{1}{2}} \right).$$

On the second step, both quantities $u_{i\pm\frac{1}{2}}^{j+\frac{1}{2}}$ can be calculated using the Lax method (2.8). As the result, following two-steps scheme is obtained (see Fig. 2.9):

$$\begin{aligned} u_{i-\frac{1}{2}}^{j+\frac{1}{2}} &= \frac{1}{2} \left(u_i^j + u_{i-1}^j \right) - \frac{c\Delta t}{2\Delta x} \left(u_i^j - u_{i-1}^j \right), \\ u_{i+\frac{1}{2}}^{j+\frac{1}{2}} &= \frac{1}{2} \left(u_i^j + u_{i+1}^j \right) - \frac{c\Delta t}{2\Delta x} \left(u_{i+1}^j - u_i^j \right), \\ u_i^{j+1} &= u_i^j - \frac{c\Delta t}{\Delta x} \left(u_{i+\frac{1}{2}}^{j+\frac{1}{2}} - u_{i-\frac{1}{2}}^{j+\frac{1}{2}} \right). \end{aligned} \quad (2.11)$$

The approximation scheme (2.11) can also be rewritten as

$$u_i^{j+1} = b_{-1}u_{i-1}^j + b_0u_i^j + b_1u_{i+1}^j, \quad (2.12)$$

where constants b_{-1} , b_0 and b_1 are given by

$$\begin{aligned} b_{-1} &= \frac{\alpha}{2}(\alpha + 1), \\ b_0 &= 1 - \alpha^2, \\ b_1 &= \frac{\alpha}{2}(\alpha - 1) \end{aligned}$$

and α is the Courant number. The matrix A of the linear system (2.6) is a sparse matrix of the form

$$A = \begin{pmatrix} b_0 & b_1 & 0 & 0 & \dots & 0 & 0 & \boxed{b_{-1}} \\ b_{-1} & b_0 & b_1 & 0 & \dots & 0 & 0 & 0 \\ 0 & b_{-1} & b_0 & b_1 & \dots & 0 & 0 & 0 \\ \dots & \dots \\ \dots & \dots \\ 0 & 0 & 0 & 0 & \dots & b_{-1} & b_0 & b_1 \\ \boxed{b_1} & 0 & 0 & 0 & \dots & 0 & b_{-1} & b_0 \end{pmatrix},$$

where boxed elements stays for influence of the periodic boundary conditions.

Notice that the three-point scheme (2.12) is second-order accurate in space and time. The distinguishing feature of the Lax–Wendroff method is, that for the linear advection equation (2.1) it is the only *explicit* scheme of second-order accuracy in space and time.

The second way to derive the Lax-Wendroff differential scheme is based on the idea that we would like to get a scheme with second-order accurate in space and time. First of all, we use Taylor series expansion in time, namely

$$u(x_i, t_{j+1}) = u(x_i, t_j) + \Delta t \partial_t u(x_i, t_j) + \frac{\Delta t^2}{2} \partial_t^2 u(x_i, t_j) + \mathcal{O}(\Delta t^3).$$

In the next place one replaces time derivatives in the last expression by space derivatives according to the relation

$$\partial_t^{(n)} u = (-c)^n \partial_x^{(n)} u.$$

Hence

$$u(x_i, t_{j+1}) = u(x_i, t_j) - c \Delta t \partial_x u(x_i, t_j) + \frac{c^2 \Delta t^2}{2} \partial_x^2 u(x_i, t_j) + \mathcal{O}(\Delta t^3).$$

Finally, the space derivatives are approximated by central differences (1.7), (1.12), resulting in the Lax-Wendroff scheme (2.12).

von Neumann stability analysis

In the case of the method (2.12) the amplification factor $g(k)$ becomes

$$g(k) = (1 + \alpha^2(\cos(k\Delta x) - 1)) - i\alpha \sin(k\Delta x)$$

and

$$|g(k)|^2 = 1 - \alpha^2(1 - \alpha^2)(1 - \cos(k\Delta x))^2.$$

Hence, the stability condition (1.22) reads

$$1 - \alpha^2 \geq 0 \Leftrightarrow \alpha = \frac{c\Delta x}{\Delta t} \leq 1,$$

and one becomes (as expected) the CFL-condition (2.7) again.

Fourier analysis

In order to check availability of dispersion, let us calculate the dispersion relation for the scheme (2.12). The ansatz of the form $\exp(i(kx_i - \omega t_j))$ results in

$$e^{-i\omega\Delta t} = (1 + \alpha^2(\cos(k\Delta x) - 1)) - i\alpha \sin(k\Delta x),$$

and with $\omega = \omega_1 - i\omega_2$ one obtains

$$\omega\Delta t = \omega_1\Delta t - i\omega_2\Delta t = i\ln\left((1 + \alpha^2(\cos(k\Delta x) - 1)) - i\alpha \sin(k\Delta x)\right).$$

One can easily see, that in the case of (2.12) dispersion (see Fig. 2.10 (a)) as well as damping (diffusion) (see Fig. 2.10 (b)) of Fourier modes take place. However, as can be seen on Fig. 2.10 and Fig. 2.11, dispersion and diffusion are weaker as for the Lax method (2.8) and appear by much smaller wave lengths. Because of these properties and taking into account the fact that the method (2.12) is of the second order, it becomes a standard scheme to approximate Eq. (2.1). Moreover, the scheme (2.12) can be generalized to the case of conservation equation in general form.

Lax-Wendroff method for 1D conservation equations

A typical one-dimensional conservation equation takes the form

$$\frac{\partial u}{\partial t} + \frac{\partial F(u)}{\partial x} = 0, \quad (2.13)$$

where $u = u(x, t)$ and the form of a function $F(u)$ depends on the problem we are interested in. One can try to apply the Lax-Wendroff method (2.12) to Eq. (2.13). With $F_i^j := F(u_i^j)$ one obtains the following differential scheme

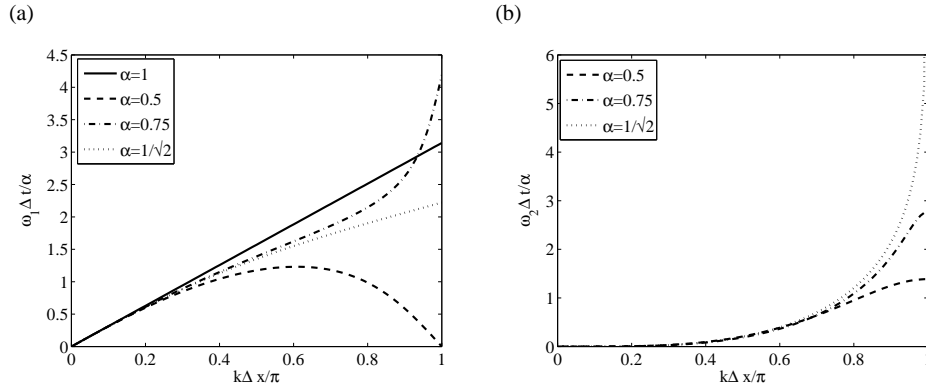


Fig. 2.10 Illustration of the dispersion relation for the Lax-Wendroff method calculated for different values of α . (a) Real part of ω (dispersion). (b) Imaginary part of ω (diffusion).

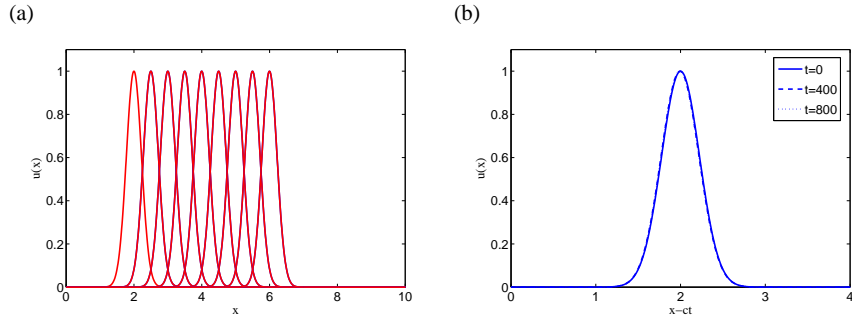


Fig. 2.11 Numerical implementation of the Lax-Wendroff method (2.12). Parameters are: Advection velocity is $c = 0.5$, length of the space interval is $L = 10$, space and time discretization steps are $\Delta x = 0.05$ and $\Delta t = 0.05$, amount of time steps is $T = 800$, and initial condition is $u_0(x) = \exp(-(x-2)^2)$. (a) Time evolution of $u(x,t)$ for different time moments. (b) Time evolution in the co-moving frame $x - ct$ at $t = 0, 400, 800$.

$$\begin{aligned}
 u_{i-\frac{1}{2}}^{j+\frac{1}{2}} &= \frac{1}{2} \left(u_i^j + u_{i-1}^j \right) - \frac{\Delta t}{2\Delta x} \left(F_i^j - F_{i-1}^j \right), \\
 u_{i+\frac{1}{2}}^{j+\frac{1}{2}} &= \frac{1}{2} \left(u_i^j + u_{i+1}^j \right) - \frac{\Delta t}{2\Delta x} \left(F_{i+1}^j - F_i^j \right), \\
 u_i^{j+1} &= u_i^j - \frac{\Delta t}{\Delta x} \left(F_{i+\frac{1}{2}}^{j+\frac{1}{2}} - F_{i-\frac{1}{2}}^{j+\frac{1}{2}} \right).
 \end{aligned} \tag{2.14}$$

Chapter 3

Burgers Equation

One of the major challenges in the field of complex systems is a thorough understanding of the phenomenon of turbulence. Direct numerical simulations (DNS) have substantially contributed to our understanding of the disordered flow phenomena inevitably arising at high Reynolds numbers. However, a successful theory of turbulence is still lacking which would allow to predict features of technologically important phenomena like turbulent mixing, turbulent convection, and turbulent combustion on the basis of the fundamental fluid dynamical equations. This is due to the fact that already the evolution equation for the simplest fluids, which are the so-called Newtonian incompressible fluids, have to take into account nonlinear as well as nonlocal properties:

$$\begin{aligned}\frac{\partial}{\partial t}\mathbf{u}(\mathbf{x},t) + \mathbf{u}(\mathbf{x},t) \cdot \nabla\mathbf{u}(\mathbf{x},t) &= -\nabla p(\mathbf{x},t) + \nu\Delta\mathbf{u}(\mathbf{x},t), \\ \nabla \cdot \mathbf{u}(\mathbf{x},t) &= 0.\end{aligned}\tag{3.1}$$

Nonlinearity stems from the convective term and the pressure term, whereas non-locality enters due to the pressure term. Due to incompressibility, the pressure is defined by a Poisson equation

$$\Delta p(\mathbf{x},t) = -\nabla \cdot \mathbf{u}(\mathbf{x},t) \cdot \nabla\mathbf{u}(\mathbf{x},t).\tag{3.2}$$

In 1939 the dutch scientist J.M. Burgers [1] simplified the Navier-Stokes equation (3.1) by just dropping the pressure term. In contrast to Eq. (3.1), this equation can be investigated in one spatial dimension (Physicists like to denote this as 1+1 dimensional problem in order to stress that there is one spatial and one temporal coordinate):

$$\frac{\partial}{\partial t}u(x,t) + u(x,t)\frac{\partial}{\partial x}u(x,t) = \nu\frac{\partial^2}{\partial x^2}u(x,t) + F(x,t)\tag{3.3}$$

Note that usually the Burgers equation is considered without external force $F(x,t)$. However, we shall include this external force field.

The Burgers equation 3.3 is nonlinear and one expects to find phenomena similar to turbulence. However, as it has been shown by Hopf [9] and Cole [3], the homogeneous Burgers equation lacks the most important property attributed to turbulence: The solutions do not exhibit chaotic features like sensitivity with respect to initial conditions. This can explicitly shown using the *Hopf-Cole transformation* which transforms Burgers equation into a linear parabolic equation. From the numerical point of view, however, this is of importance since it allows one to compare numerically obtained solutions of the nonlinear equation with the exact one. This comparison is important to investigate the quality of the applied numerical schemes. Furthermore, the equation has still interesting applications in physics and astrophysics. We will briefly mention some of them.

Growth of interfaces: Deposition models

The Burgers equation (3.3) is equivalent to the so-called *Kardar-Parisi-Zhang (KPZ-) equation* which is a model for a solid surface growing by vapor deposition, or, the opposite case, erosion of material from a solid surface. The location of the surface is described in terms of a height function $h(\mathbf{x}, t)$. This height evolves in time according to the KPZ-equation

$$\frac{\partial}{\partial t} h(\mathbf{x}, t) - \frac{1}{2} (\nabla h(\mathbf{x}, t))^2 = \nu \frac{\partial^2}{\partial x^2} h(x, t) + F(x, t). \quad (3.4)$$

This equation is obtained from the simple advection equation for a surface at $z = h(\mathbf{x}, t)$ moving with velocity $\mathbf{U}(\mathbf{x}, t)$

$$\frac{\partial}{\partial t} h(\mathbf{x}, t) + \mathbf{U} \cdot \nabla h(\mathbf{x}, t) = 0. \quad (3.5)$$

The velocity is assumed to be proportional to the gradient of $h(\mathbf{x}, t)$, i.e. the surface evolves in the direction of its gradient. Surface diffusion is described by the diffusion term.

Burgers equation (3.3) is obtained from the KPZ-equation just by forming the gradient of $h(\mathbf{x}, t)$:

$$\mathbf{u}(\mathbf{x}, t) = -\nabla h(\mathbf{x}, t). \quad (3.6)$$

3.1 Hopf-Cole Transformation

The Hopf-Cole transformation is a transformation, which maps the solution of the Burgers equation (3.3) to the heat equation

$$\frac{\partial}{\partial t} \psi(\mathbf{x}, t) = \nu \Delta \psi(\mathbf{x}, t). \quad (3.7)$$

We perform the ansatz

$$\psi(\mathbf{x}, t) = e^{h(\mathbf{x}, t)/2\nu} \quad (3.8)$$

and determine

$$\Delta\psi = \frac{1}{2\nu} \left[\Delta h + \frac{1}{2\nu} (\nabla h)^2 \right] e^{h/2\nu} \quad (3.9)$$

leading to

$$\frac{\partial}{\partial t} h - \frac{1}{2} (\nabla h)^2 = \nu \Delta h. \quad (3.10)$$

However, this is exactly the Kardar-Parisi-Zhang equation (3.4). The complete transformation is then obtained by combining

$$\mathbf{u}(\mathbf{x}, t) = -\frac{1}{2\nu} \nabla \ln \psi(\mathbf{x}, t). \quad (3.11)$$

We explicitly see that the Hopf-Cole transformation turns the nonlinear Burgers equation into the linear heat conduction equation. Since the heat conduction equation is explicitly solvable in terms of the so-called heat kernel we obtain a general solution of the Burgers equation. Before we construct this general solution, we want to emphasize that the Hopf-Cole transformation applied to the multi-dimensional Burgers equation only leads to the general solution provided the initial condition $\mathbf{u}(\mathbf{x}, 0)$ is a gradient field. For general initial conditions, especially for initial fields with $\nabla \times \mathbf{u}(\mathbf{x}, t)$, the solution can not be constructed using the Hopf-Cole transformation and, consequently, is not known in analytical terms. In one dimension spatial dimension it is not necessary to distinguish between these two cases.

3.2 General Solution of the 1D Burgers Equation

We are now in the position to formulate the general solution of the Burgers equation (3.3) in one spatial dimension with initial condition

$$u(x, 0), \quad \psi(x, 0) = e^{-\frac{1}{2\nu} \int^x dx' u(x', 0)}. \quad (3.12)$$

The solution of the 1D heat equation can be expressed by the heat-kernel

$$\psi(x, t) = \int dx' G(x - x', t) \psi(x', 0) \quad (3.13)$$

with the kernel

$$G(x - x', t) = \frac{1}{\sqrt{4\pi t}} e^{-\frac{(x-x')^2}{4\nu t}} \quad (3.14)$$

In terms of the initial condition (3.12) the solution explicitly reads

$$\psi(x, t) = \frac{1}{\sqrt{4\pi t}} \int dx' e^{-\frac{(x-x')^2}{4\nu t} - \frac{1}{2\nu} \int^{x'} dx'' u(x'', 0)}. \quad (3.15)$$

The n -dimensional solution of the Burgers equation (3.3) for initial fields, which are gradient fields, are obtained analogously:

$$\psi(x, t) = \frac{1}{(4\pi t)^{d/2}} \int d\mathbf{x}' e^{-\frac{(\mathbf{x}-\mathbf{x}')^2}{4vt}} - \frac{1}{2v} \int^{\mathbf{x}'} d\mathbf{x}'' \cdot \mathbf{u}(\mathbf{x}'', 0). \quad (3.16)$$

Again, we see that the solution exist provided the integral is independent of the integration contour:

$$\int^{\mathbf{x}'} d\mathbf{x}'' \cdot \mathbf{u}(\mathbf{x}'', 0) = h(\mathbf{x}', t). \quad (3.17)$$

We can investigate the limiting case of vanishing viscosity, $v \rightarrow 0$. In the expression for $\psi(x, t)$, eq. (3.16), the integral is dominated by the minimum of the exponential function,

$$\min_{x'} \left[-\frac{(x-x')^2}{4vt} - \frac{1}{2v} \int^{x'} dx'' u(x'', 0) \right]. \quad (3.18)$$

This leads to the so-called characteristics (see App. (B))

$$x = x' - tu(x', 0), \quad (3.19)$$

which we have already met in the discussion of the advection equation (2.1) (see Chapter 2). A special solution for the viscid Burgers equation is

$$u(x, t) = 1 - \tanh\left(\frac{x - x_c - t}{2v}\right). \quad (3.20)$$

3.3 Forced Burgers Equation

The Hopf-Cole transformation can be applied to the forced Burgers equation. It is straightforward to show that this leads to the parabolic differential equation

$$\frac{\partial}{\partial t} \psi(x, t) = v \Delta \psi(\mathbf{x}, t) - U(\mathbf{x}, t) \psi(\mathbf{x}, t), \quad (3.21)$$

where the potential is related to the force

$$\mathbf{F}(\mathbf{x}, t) = -\frac{1}{2v} \nabla U(\mathbf{x}, t). \quad (3.22)$$

The relationship with the Schrödinger equation for a particle moving in the potential $U(\mathbf{x}, t)$ is obvious. Recently, the Burgers equation with a fluctuating force has been investigated [14]. Interestingly, Burgers equation with a linear force, i.e. a quadratic potential

$$U(x, t) = a(t)x^2 \quad (3.23)$$

for an arbitrary time dependent coefficient $a(t)$ could be solved analytically [8].

3.4 Numerical Treatment

Let us consider a one-dimensional Burgers equation (3.3) without forcing.

$$\frac{\partial u}{\partial t} + u \frac{\partial u}{\partial x} = \nu \frac{\partial^2 u}{\partial x^2}.$$

When $\nu = 0$, Burgers equation becomes *the inviscid Burgers equation*:

$$\frac{\partial u}{\partial t} + u \frac{\partial u}{\partial x} = 0, \quad (3.24)$$

which is a prototype for equations for which the solution can develop discontinuities (*shock waves*). As was mentioned above, as the solution of the advection equation (2.1), the solution of Eq. (3.24) can be constructed by the method of characteristics (see App. B). Suppose we have an initial value problem, i.e., a smooth function $u(x, 0) = u_0(x)$, $x \in \mathbb{R}$ is given. In this case the coefficients A , B and C are

$$A = u, \quad B = 1, \quad C = 0.$$

Equations (B.2-B.3) read

$$\begin{aligned} \frac{dt}{ds} &= 1 \Leftrightarrow |t(0) = 0| \Leftrightarrow t = s, \\ \frac{du}{ds} &= 0 \Leftrightarrow |u(0) = u_0(x_0)| \Leftrightarrow u(s, x_0) = u_0(x_0), \\ \frac{dx}{ds} &= u \Leftrightarrow |x(0) = x_0| \Leftrightarrow x = u_0(x_0)t + x_0. \end{aligned}$$

Hence the general solution of (3.24) takes the form

$$u(x, t) = u_0(x - u_0(x_0)t, t). \quad (3.25)$$

Eq. (3.25) is an implicit relation that determines the solution of the inviscid Burgers' equation. Note that the characteristics are straight lines, but not all the lines have the same slope. It will be possible for the characteristics to intersect. If we write the characteristics as

$$t = \frac{x}{u_0(x_0)} - \frac{x_0}{u_0(x_0)},$$

one can see, that the slope $1/u_0(x_0)$ of the characteristics depends on the point x_0 and on the initial function u_0 . For inviscid Burgers' equation (3.24), the time T_c at which the characteristics cross and a shock forms, the "breaking" time, can be determined exactly as

$$T_c = \frac{-1}{\min\{u_x(x, 0)\}}$$

This relation can be used if Eq. (3.24) has smooth initial data (so that it is differentiable). From the formula for T_c , we can see that the solution will break and a shock

will form if $u_x(x, 0)$ is negative at some point.

From numerical point of view it is convenient to rewrite the Burgers' equation as

$$\frac{\partial u}{\partial t} + \frac{1}{2} \frac{\partial}{\partial x}(u^2) = 0 \quad (3.26)$$

Equation (3.26) describes a one-dimensional conservation law (2.13) with $F = \frac{1}{2}u^2$ and can be solve, e.g., with the upwind method (2.4) or with the Lax-Wendroff method (2.14).

Space interval	$L=10$
Initial condition	$u_0(x) = \exp(-(x-3)^2)$
Space discretization step	$\Delta x = 0.05$
Time discretization step	$\Delta t = 0.05$
Amount of time steps	$T = 36$

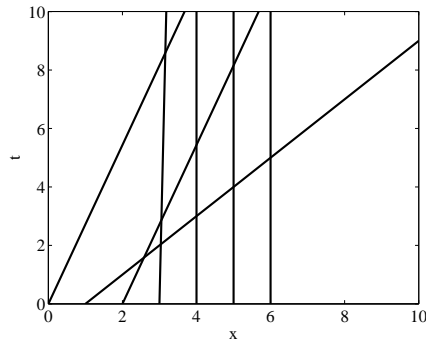


Fig. 3.1 Characteristics curves for the inviscid Burgers' equation (3.24)

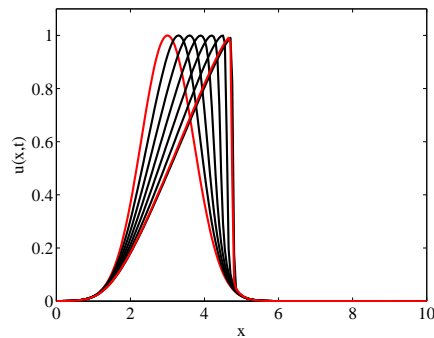


Fig. 3.2 Numerical solution of the inviscid Burgers' equation (3.24)

3.4.0.1 The Riemann Problem

A Riemann problem, named after *Bernhard Riemann*, consists of a conservation law, e.g., Eq. (3.24) together with a piecewise constant data having a single discontinuity, i.e.,

$$u(x,0) = u_0(x) = \begin{cases} u_l, & x < a; \\ u_r, & x \geq a. \end{cases} \quad (3.27)$$

The form of the solution depends on the relation between u_l and u_r .

- $u_l > u_r$: The unique weak solution (see Fig. 3.2 (a)) is

$$u(x,0) = u_0(x) = \begin{cases} u_l, & x < a + ct; \\ u_r, & x \geq a + ct \end{cases} \quad (3.28)$$

with the *shock velocity*

$$c = \frac{1}{2}(u_l + u_r).$$

Note, that in this case the characteristics in each of the region where u is constant go into the shock as time advances (see Fig. 3.3 (b)).

Space interval	$L=10$
Initial condition	$u_l = 0.8, u_r = 0.2$
Space discretization step	$\Delta x = 0.05$
Time discretization step	$\Delta t = 0.05$
Amount of time steps	$T = 100$

The initial condition is:

$$u(x,0) = u_0(x) = \begin{cases} 0.8, & x < 5; \\ 0.2, & x \geq 5. \end{cases} \quad (3.29)$$

- $u_l < u_r$: In this case there are infinitely many weak solutions. One of them is again (3.28) with the same velocity (see Fig. 3.4 (a)). Note that in this case the characteristics go out of the shock (Fig. 3.4 (b)) and the solution is not stable to perturbations.

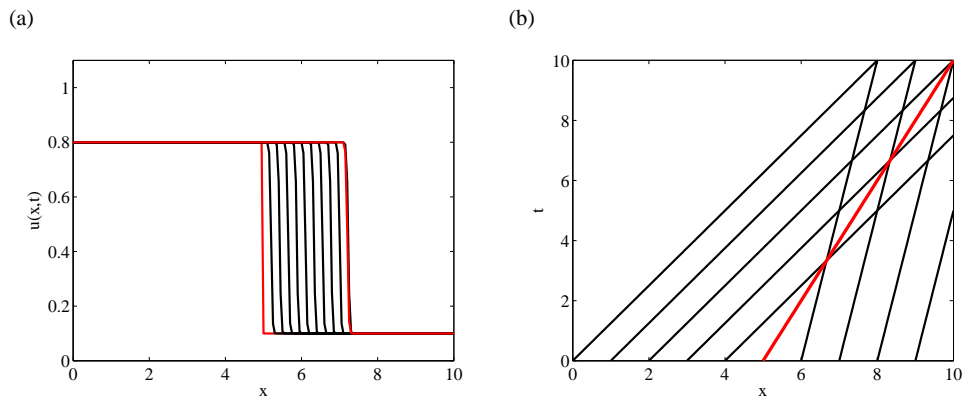


Fig. 3.3 a) Numerical solution of the inviscid Burgers' equation (3.24) for the Riemann problem for $u_l < u_r$. b) Characteristics of Eq. (3.24) with initial conditions (3.29). The red line indicates the curve $x = a + ct$.

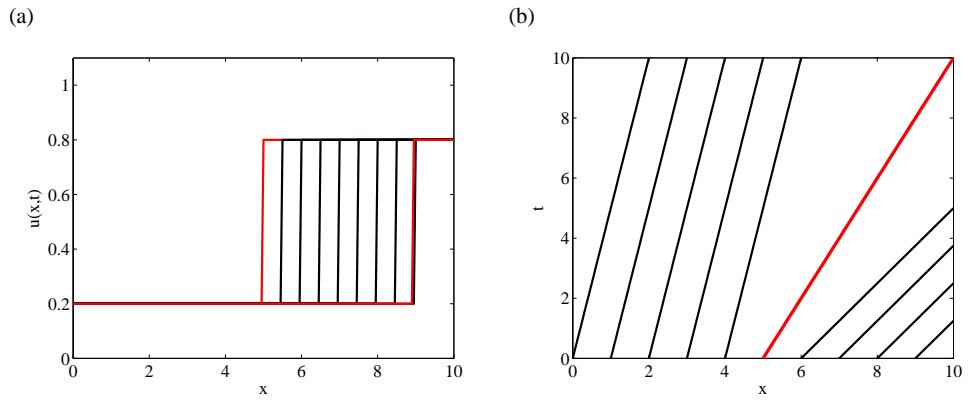


Fig. 3.4 a) Numerical solution of the inviscid Burgers' equation (??) for the Riemann problem for $u_l < u_r$. b) Characteristics of the inviscid Burgers' equation with initial conditions (??). The red line indicates the curve $x = a + ct$.

Chapter 4

The Wave Equation

Another classical example of a hyperbolic PDE is a wave equation. The wave equation is a second-order linear hyperbolic PDE that describes the propagation of a variety of waves, such as sound or water waves. It arises in different fields such as acoustics, electromagnetics, or fluid dynamics. In its simplest form, the wave equation refers to a scalar function $u = u(\mathbf{r}, t)$, $\mathbf{r} \in \mathbb{R}^n$ that satisfies:

$$\frac{\partial^2 u}{\partial t^2} = c^2 \nabla^2 u. \quad (4.1)$$

Here ∇^2 denotes the Laplacian in \mathbb{R}^n and c is a constant speed of the wave propagation. An even more compact form of Eq. (4.1) is given by

$$\square u = 0,$$

where $\square = \nabla^2 - \frac{1}{c^2} \frac{\partial^2}{\partial t^2}$ is the d'Alembertian.

4.1 The Wave Equation in 1D

The wave equation for the scalar u in the one dimensional case reads

$$\frac{\partial^2 u}{\partial t^2} = c^2 \frac{\partial^2 u}{\partial x^2}. \quad (4.2)$$

The one-dimensional wave equation (4.2) can be solved exactly by d'Alembert's method, using a Fourier transform method, or via separation of variables. To illustrate the idea of the d'Alembert method, let us introduce new coordinates (ξ, η) by use of the transformation

$$\xi = x - ct, \quad \eta = x + ct. \quad (4.3)$$

In the new coordinate system one can write

$$u_{xx} = u_{\xi\xi} + 2u_{\xi\eta} + u_{\eta\eta}, \quad \frac{1}{c^2}u_{tt} = u_{\xi\xi} - 2u_{\xi\eta} + u_{\eta\eta},$$

and Eq. (4.2) becomes

$$\frac{\partial^2 u}{\partial \xi \partial \eta} = 0. \quad (4.4)$$

That is, the function u remains constant along the curves (4.3), i.e., Eq. (4.3) describes characteristic curves of the wave equation (4.2) (see App. B). Moreover, one can see that the derivative $\partial u / \partial \xi$ does not depend on η , i.e.,

$$\frac{\partial}{\partial \eta} \left(\frac{\partial u}{\partial \xi} \right) = 0 \Leftrightarrow \frac{\partial u}{\partial \xi} = f(\xi).$$

After integration with respect to ξ one obtains

$$u(\xi, \eta) = F(\xi) + G(\eta),$$

where F is the primitive function of f and G is the "constant" of integration, in general the function of η . Turning back to the coordinates (x, t) one obtains the general solution of Eq. (4.2)

$$\boxed{u(x, t) = F(x - ct) + G(x + ct)}. \quad (4.5)$$

4.1.1 Solution of the IVP

Now let us consider an initial value problem for Eq. (4.2):

$$\begin{aligned} u_{tt} &= c^2 u_{xx}, \quad t \geq 0, \\ u(x, 0) &= f(x), \\ u_t(x, 0) &= g(x). \end{aligned} \quad (4.6)$$

To write down the general solution of the IVP for Eq. (4.2), one needs to express the arbitrary function F and G in terms of initial data f and g . Using the relation

$$\frac{\partial}{\partial t} F(x - ct) = -c F'(x - ct), \quad \text{where} \quad F'(x - ct) := \frac{\partial}{\partial \xi} F(\xi)$$

one becomes:

$$\begin{aligned} u(x, 0) &= F(x) + G(x) = f(x); \\ u_t(x, 0) &= c(-F'(x) + G'(x)) = g(x). \end{aligned}$$

After differentiation of the first equation with respect to x one can solve the system in terms of $F'(x)$ and $G'(x)$, i.e.,

$$F'(x) = \frac{1}{2} \left(f'(x) - \frac{1}{c} g(x) \right), \quad G'(x) = \frac{1}{2} \left(f'(x) + \frac{1}{c} g(x) \right).$$

Hence

$$F(x) = \frac{1}{2} f(x) - \frac{1}{2c} \int_0^x g(y) dy + C, \quad G(x) = \frac{1}{2} f(x) + \frac{1}{2c} \int_0^x g(y) dy - C,$$

where the integration constant C is chosen in such a way that the initial condition $F(x) + G(x) = f(x)$ is fulfilled. Altogether one obtains:

$$u(x, t) = \frac{1}{2} \left(f(x - ct) + f(x + ct) \right) + \frac{1}{2c} \int_{x-ct}^{x+ct} g(y) dy. \quad (4.7)$$

4.1.2 Numerical Treatment

4.1.2.1 A Simple Explicit Method

The first idea is just to use central differences for both time and space derivatives, i.e.,

$$\frac{u_i^{j+1} - 2u_i^j + u_i^{j-1}}{\Delta t^2} = c^2 \frac{u_{i+1}^j - 2u_i^j + u_{i-1}^j}{\Delta x^2}, \quad (4.8)$$

or, with $\alpha = c\Delta t/\Delta x$

$$u_i^{j+1} = -u_i^{j-1} + 2(1 - \alpha^2)u_i^j + \alpha^2(u_{i+1}^j + u_{i-1}^j). \quad (4.9)$$

Schematical representation of the scheme (4.9) is shown on Fig. 4.1.

Note that one should also implement initial conditions (4.6). In order to implement the second initial condition one needs the virtual point u_i^{-1} ,

$$u_t(x_i, 0) = g(x_i) = \frac{u_i^1 - u_i^{-1}}{2\Delta t} + \mathcal{O}(\Delta t^2).$$

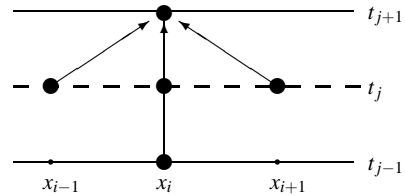


Fig. 4.1 Schematical visualization of the numerical scheme (4.9) for (4.2).

With $g_i := g(x_i)$ one can rewrite the last expression as

$$u_i^{-1} = u_i^1 - 2\Delta t g_i + \mathcal{O}(\Delta t^2),$$

and the second time row can be calculated as

$$\boxed{u_i^1 = \Delta t g_i + (1 - \alpha^2)f_i + \frac{1}{2}\alpha^2(f_{i-1} + f_{i+1})}, \quad (4.10)$$

where $u(x_i, 0) = u_i^0 = f(x_i) = f_i$.

von Neumann Stability Analysis

In order to investigate the stability of the explicit scheme (4.9) we start with the usual ansatz (1.21)

$$\varepsilon_i^j = g^j e^{ikx_i},$$

which leads to the following expression for the amplification factor $g(k)$

$$g^2 = 2(1 - \alpha^2)g - 1 + 2\alpha^2 g \cos(k\Delta x).$$

After several transformations the last expression becomes just a quadratic equation for g , namely

$$g^2 - 2\beta g + 1 = 0, \quad (4.11)$$

where

$$\beta = 1 - 2\alpha^2 \sin^2\left(\frac{k\Delta x}{2}\right).$$

Solutions of the equation for $g(k)$ read

$$g_{1,2} = \beta \pm \sqrt{\beta^2 - 1}.$$

Notice that if $|\beta| > 1$ then at least one of absolute value of $g_{1,2}$ is bigger than one. Therefore one should desire for $|\beta| < 1$, i.e.,

$$g_{1,2} = \beta \pm i\sqrt{\beta^2 - 1}$$

and

$$|g|^2 = \beta^2 + 1 - \beta^2 = 1.$$

That is, the scheme (4.9) is conditional stable. The stability condition reads

$$-1 \leq 1 - 2\alpha^2 \sin^2\left(\frac{k\Delta x}{2}\right) \leq 1,$$

what is equivalent to the standart CFL condition (2.7)

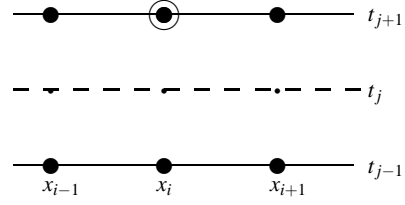


Fig. 4.2 Schematic visualization of the implicit numerical scheme (4.12) for (4.2).

$$\alpha = \frac{c\Delta t}{\Delta x} \leq 1.$$

4.1.2.2 An Implicit Method

One can try to overcome the problems with conditional stability by introducing *an implicit scheme*. The simplest way to do it is just to replace all terms on the right hand side of (4.8) by an average from the values to the time steps $j + 1$ and $j - 1$, i.e.,

$$\frac{u_i^{j+1} - 2u_i^j + u_i^{j-1}}{\Delta t^2} = \frac{c^2}{2\Delta x^2} \left(u_{i+1}^{j-1} - 2u_i^{j-1} + u_{i-1}^{j-1} + u_{i+1}^{j+1} - 2u_i^{j+1} + u_{i-1}^{j+1} \right). \quad (4.12)$$

Schematic diagramm of the numerical scheme (4.12) is shown on Fig. (4.2).

Let us check the stability of the implicit scheme (4.12). To this aim we use the standart ansatz

$$\varepsilon_i^j = g^j e^{ikx_i}$$

leading to the equation for $g(k)$

$$\beta g^2 - 2g + \beta = 0$$

with

$$\beta = 1 + 2\alpha^2 \sin^2\left(\frac{k\Delta x}{2}\right).$$

One can see that $\beta \geq 1$ for all k . Hence the solutions $g_{1,2}$ take the form

$$g_{1,2} = \frac{1 \pm i\sqrt{1 - \beta^2}}{\beta}$$

and

$$|g|^2 = \frac{1 - (1 - \beta^2)}{\beta^2} = 1.$$

That is, the implicit scheme (4.12) is *absolute stable*.

Now, the question is, whether the implicit scheme (4.12) is better than the explicit scheme (4.9) form numerical point of view. To answer this question, let us analyse dispersion relation for the wave equation (4.2) as well as for both schemes (4.9) and

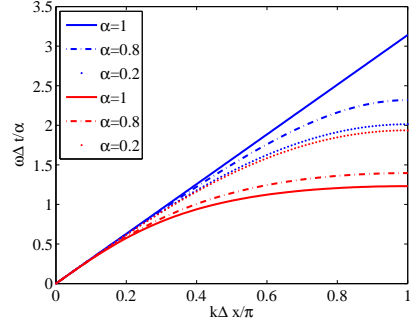


Fig. 4.3 Dispersion relation for the one-dimensional wave equation (4.2), calculated using the explicit (blue curves) and implicit (red curves) methods (4.9) and (4.12).

(4.12). The exact dispersion relation is

$$\omega = \pm ck,$$

i.e, all Fourier modes propagate without dispersion with the same phase velocity $\omega/k = \pm c$. Using the ansatz $u_i^j \sim e^{ikx_i - i\omega t_j}$ for the explicit method (4.9) one obtains:

$$\cos(\omega\Delta t) = 1 - \alpha^2(1 - \cos(k\Delta x)), \quad (4.13)$$

while for the implicit method (4.12)

$$\cos(\omega\Delta t) = \frac{1}{1 + \alpha^2(1 - \cos(k\Delta x))}. \quad (4.14)$$

One can see that for $\alpha \rightarrow 0$ both methods provide the same result, otherwise the explicit scheme (4.9) always exceeds the implicit one (see Fig. (4.3)). For $\alpha = 1$ the scheme (4.9) becomes exact, while (4.12) deviates more and more from the exact value of ω for increasing α . Hence, for Eq. (4.2) there are no motivation to use implicit scheme instead of the explicit one.

4.1.3 Examples

Example 1.

Use the explicit method (4.9) to solve the one-dimansional wave equation (4.2):

$$u_{tt} = 4u_{xx} \quad \text{for } x \in [0, L] \quad \text{and } t \in [0, T] \quad (4.15)$$

with boundary conditions

$$u(0, t) = 0 \quad u(L, t) = 0.$$

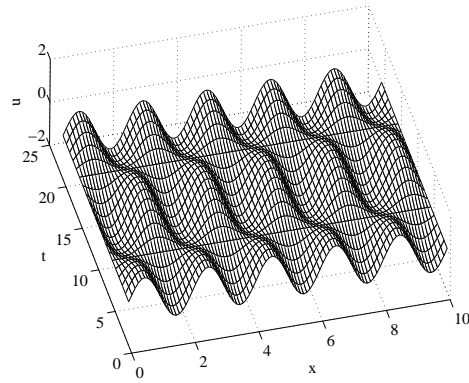


Fig. 4.4 Space-time evolution of Eq. (4.15) with the initial distribution $u(x, 0) = \sin(\pi x)$, $u_t(x, 0) = 0$.

Assume that the initial position and velocity are

$$u(x, 0) = f(x) = \sin(\pi x), \quad \text{and} \quad u_t(x, 0) = g(x) = 0.$$

Other parameters are:

$$\begin{array}{l} \text{Space interval} \\ \text{Space discretization step} \\ \text{Time discretization step} \\ \text{Amount of time steps} \end{array} \left\| \begin{array}{l} L=10 \\ \Delta x = 0.1 \\ \Delta t = 0.05 \\ T = 20 \end{array} \right.$$

First one can find the d'Alambert solution. In the case of zero initial velocity Eq. (4.7) becomes

$$u(x, t) = \frac{f(x-2t) + f(x+2t)}{2} = \frac{\sin \pi(x-2t) + \sin \pi(x+2t)}{2} = \sin(\pi x) \cos(2\pi t),$$

i.e., the solution is just a sum of a travelling waves with initial form, given by $\frac{f(x)}{2}$. Numerical solution of (4.15) is shown on Fig. (4.4).

Example 2.

Solve Eq. (4.15) with the same boundary conditions. Assume now, that initial distributions of position and velocity are

$$u(x, 0) = f(x) = 0 \quad \text{and} \quad u_t(x, 0) = g(x) = \begin{cases} 0, & x \in [0, x_1]; \\ g_0, & x \in [x_1, x_2]; \\ 0, & x \in [x_2, L]. \end{cases}$$

Other parameters are:

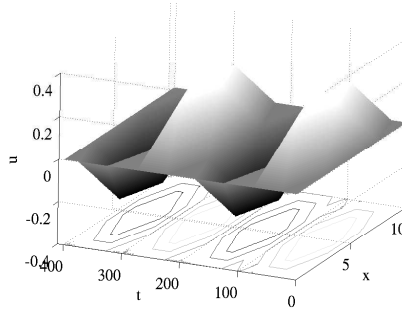


Fig. 4.5 Space-time evolution of Eq. (4.15) with the initial distribution $u(x, 0) = 0$, $u_t(x, 0) = g(x)$.

Initial nonzero velocity	$g_0=0.5$
Initial space intervals	$x_1 = L/4, x_2 = 3L/4$
Space interval	$L=10$
Space discretization step	$\Delta x = 0.1$
Time discretization step	$\Delta t = 0.05$
Amount of time steps	$T = 400$

Numerical solution of the problem is shown on Fig. (4.5).

Example 3. Vibrating String

Use the explicit method (4.9) to solve the wave equation for a vibrating string:

$$u_{tt} = c^2 u_{xx} \quad \text{for } x \in [0, L] \quad \text{and } t \in [0, T], \quad (4.16)$$

where $c = 1$ with the boundary conditions

$$u(0, t) = 0 \quad u(L, t) = 0.$$

Assume that the initial position and velocity are

$$u(x, 0) = f(x) = \sin(n\pi x/L), \quad \text{and } u_t(x, 0) = g(x) = 0, \quad n = 1, 2, 3, \dots$$

Other parameters are:

Space interval	$L=1$
Space discretization step	$\Delta x = 0.01$
Time discretization step	$\Delta t = 0.0025$
Amount of time steps	$T = 2000$

Usually a vibrating string produces a sound whose frequency is constant. Therefore, since frequency characterizes the pitch, the sound produced is a constant note. Vibrating strings are the basis of any string instrument like guitar or cello. If the speed of propagation c is known, one can calculate the frequency of the sound pro-

duced by the string. The speed of propagation of a wave c is equal to the wavelength multiplied by the frequency f :

$$c = \lambda f$$

If the length of the string is L , the fundamental harmonic is the one produced by the vibration whose nodes are the two ends of the string, so L is half of the wavelength of the fundamental harmonic, so

$$f = \frac{c}{2L}$$

Solutions of the equation in question are given in form of standing waves. The standing wave is a wave that remains in a constant position. This phenomenon can occur because the medium is moving in the opposite direction to the wave, or it can arise in a stationary medium as a result of interference between two waves traveling in opposite directions (see Fig. (4.6))

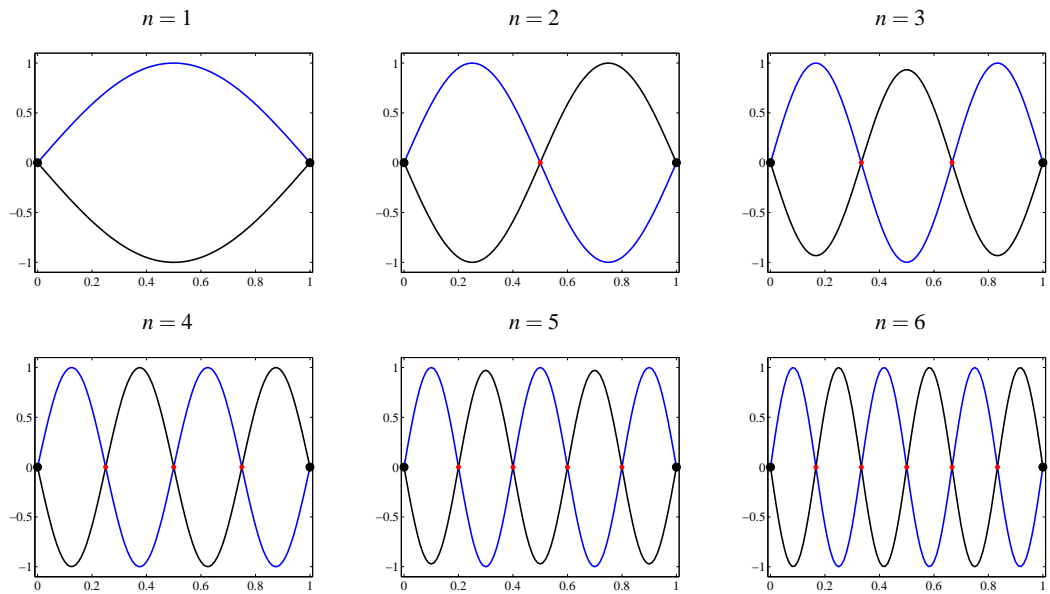


Fig. 4.6 Standing waves in a string. The fundamental mode and the first five overtones are shown. The red dots represent the wave nodes.

4.2 The Wave Equation in 2D

4.2.1 Examples

4.2.1.1 Example 1.

Use the standard five-point explicit method (4.9) to solve a two-dimensional wave equation

$$u_{tt} = c^2(u_{xx} + u_{yy}), \quad u = u(x, y, t)$$

on the rectangular domain $[0, L] \times [0, L]$ with Dirichlet boundary conditions. Other parameters are:

Space interval	$L=1$
Space discretization step	$\Delta x = \Delta y = 0.01$
Time discretization step	$\Delta t = 0.0025$
Amount of time steps	$T = 2000$
Initial condition	$u(x, y, 0) = 4x^2y(1-x)(1-y)$

Numerical solution of the problem for two different time moments $t = 0$ and $t = 500$ can be seen on Fig. (4.7)

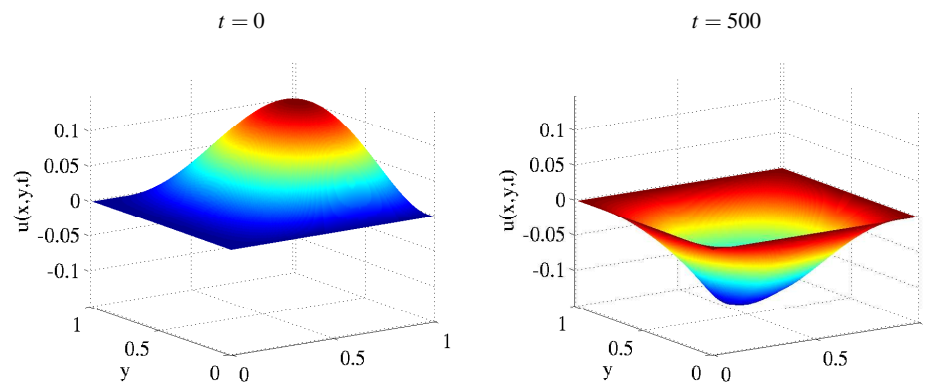


Fig. 4.7 Numerical solution of the two-dimensional wave equation, shown for $t = 0$ and $t = 500$.

Chapter 5

Sine-Gordon Equation

The sine-Gordon equation is a nonlinear hyperbolic partial differential equation involving the d'Alembert operator and the sine of the unknown function. The equation, as well as several solution techniques, were known in the nineteenth century in the course of study of various problems of differential geometry. The equation grew greatly in importance in the 1970s, when it was realized that it led to *solitons* (so-called "kink" and "antikink"). The sine-Gordon equation appears in a number of physical applications [11, 7, 21], including applications in relativistic field theory, Josephson junctions [17] or mechanical transmission lines [18, 17].

The equation reads

$$u_{tt} - u_{xx} + \sin u = 0, \quad (5.1)$$

where $u = u(x, t)$. In the case of mechanical transmission line, $u(x, t)$ describes an angle of rotation of the pendulums. Note that in the low-amplitude case ($\sin u \approx u$) Eq. (5.1) reduces to the Klein-Gordon equation

$$u_{tt} - u_{xx} + u = 0,$$

admitting solutions in the form

$$u(x, t) = u_0 \cos(kx - \omega t), \quad \omega = \sqrt{1 + k^2}.$$

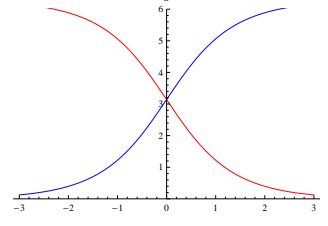
Here we are interested in large amplitude solutions of Eq. (5.1).

5.1 Kink and antikink solitons

Let us look for travelling wave solutions of the sine-Gordon equation (5.1) of the form

$$u(\xi) := u(x - ct),$$

Fig. 5.1 Representation of the kink (blue) and antikink (red) solutions (5.4)



where c is an arbitrary velocity of propagation and $u \rightarrow 0$, $u_\xi \rightarrow 0$, when $\xi \rightarrow \pm\infty$ [17, 21]. In the co-moving frame Eq. (5.1) reads

$$(1 - c^2)u_{\xi\xi} = \sin u.$$

Multiplying both sides of the last equation by u_ξ and integrating yields

$$\frac{1}{2}u_\xi^2(1 - c^2) = -\cos u + c_1, \quad (5.2)$$

where c_1 is an arbitrary constant of integration. Notice that we look for solutions for which $u \rightarrow 0$ and $u_\xi \rightarrow 0$ when $\xi \rightarrow \pm\infty$, so $c_1 = 1$. Now we can rewrite the last equation as

$$\frac{du}{\sin \frac{u}{2}} = \pm \frac{2}{\sqrt{1 - c^2}} d\xi. \quad (5.3)$$

Integrating Eq. (5.3) yields

$$\pm \frac{2}{\sqrt{1 - c^2}} (\xi - \xi_0) = 2 \ln \left(\tan \frac{u}{4} \right),$$

or

$$u(\xi) = 4 \arctan \left(\exp \left(\pm \frac{\xi - \xi_0}{\sqrt{1 - c^2}} \right) \right).$$

That is, the solution of Eq. (5.1) becomes

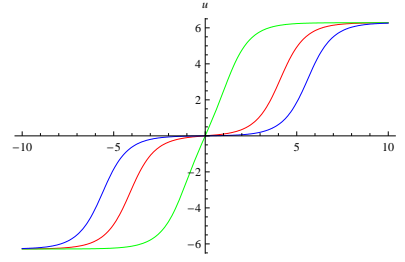
$$u(x, t) = 4 \arctan \left(\exp \left(\pm \frac{x - x_0 - ct}{\sqrt{1 - c^2}} \right) \right). \quad (5.4)$$

Equation (5.4) represents a localized solitary wave, travelling at any velocity $|c| < 1$. The \pm signs correspond to localized solutions which are called *kink* and *antikink*, respectively. For the mechanical transmission line, when c increases from $-\infty$ to $+\infty$ the pendulums rotate from 0 to 2π for the kink and from 0 to -2π for the antikink. (see Fig. 5.1)

One can show [11, 17], that Eq. (5.1) admits more solutions of the form

$$u(x, t) = 4 \arctan \left(\frac{F(x)}{G(t)} \right).$$

Fig. 5.2 The kink-kink collision, calculated at three different times: At $t = -7$ (red curve) both kinks propagate with opposite velocities $c = \pm 0.5$; At $t = 0$ they collide at the origin (green curve); At $t = 10$ (blue curve) they move away from the origin with velocities $c = \mp 0.5$.



where F and G are arbitrary functions. Namely, one distinguishes the kink-kink and the kink-antikink collisions as well as the breather solution. The *kink-kink collision* solution reads

$$u(x, t) = 4 \arctan\left(\frac{c \sinh\left(\frac{x}{\sqrt{1-c^2}}\right)}{\cosh\left(\frac{ct}{\sqrt{1-c^2}}\right)}\right) \quad (5.5)$$

and describes the collision between two kinks with respective velocities c and $-c$ and approaching the origin from $t \rightarrow -\infty$ and moving away from it with velocities $\pm c$ for $t \rightarrow \infty$ (see Fig. 5.2). In a similar way, one can construct solution, corresponding to the *kink-antikink collision*. The solution has the form:

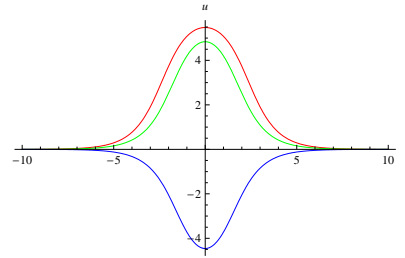
$$u(x, t) = 4 \arctan\left(\frac{\sinh\left(\frac{ct}{\sqrt{1-c^2}}\right)}{c \cdot \cosh\left(\frac{x}{\sqrt{1-c^2}}\right)}\right) \quad (5.6)$$

The *breather* soliton solution, which is also called a *breather mode* or *breather soliton* [17], is given by

$$u_B(x, t) = 4 \arctan\left(\frac{\sqrt{1-\omega^2} \sin(\omega t)}{\omega \cosh(\sqrt{1-\omega^2} x)}\right) \quad (5.7)$$

which is periodic for frequencies $\omega < 1$ and decays exponentially when moving away from $x = 0$. Now we are in the good position to look for numerical solutions

Fig. 5.3 The breather solution, oscillating with the frequency $\omega = 0.2$, calculated for three different times $t = 0$ (red curve), $t = 5$ (green curve) and $t = 10$ (blue curve).



of Eq. (5.1).

5.2 Numerical treatment

A numerical scheme

Consider an IVP for the sine-Gordon equation (5.1):

$$u_{tt} - u_{xx} + \sin(u) = 0$$

on the interval $x \in [a, b]$ with initial conditions

$$u(x, 0) = f(x), \quad u_t(x, 0) = g(x), \quad (5.8)$$

and with, e.g., no-flux boundary conditions

$$\left. \frac{\partial u}{\partial x} \right|_{x=a,b} = 0.$$

Let us try to apply a simple explicit scheme (4.9) to Eq. (5.1). The discretization scheme reads

$$u_i^{j+1} = -u_i^{j-1} + 2(1 - \alpha^2)u_i^j + \alpha^2(u_{i+1}^j + u_{i-1}^j) - \Delta t^2 \sin(u_i^j) \quad (5.9)$$

with $\alpha = \Delta t / \Delta x$, $i = 0, \dots, M$ and $t = 0, \dots, T$. To the implementation of the second initial condition one needs again the virtual point u_i^{-1} ,

$$u_t(x_i, 0) = g(x_i) = \frac{u_i^1 - u_i^{-1}}{2\Delta t} + \mathcal{O}(\Delta t^2).$$

Hence, one can rewrite the last expression as

$$u_i^{-1} = u_i^1 - 2\Delta t g(x_i) + \mathcal{O}(\Delta t^2),$$

and the second time row u_i^1 can be calculated as

$$u_i^1 = \Delta t g(x_i) + (1 - \alpha^2)f(x_i) + \frac{1}{2}\alpha^2(f(x_{i-1}) + f(x_{i+1})) - \frac{\Delta t^2}{2}\sin(f(x_i)). \quad (5.10)$$

In addition, no-flux boundary conditions lead to the following expressions for two virtual space points u_{-1}^j and u_{M+1}^j :

$$\begin{aligned} \left. \frac{\partial u}{\partial x} \right|_{x=a} = 0 &\Leftrightarrow \frac{u_1^j - u_{-1}^j}{2\Delta x} = 0 \Leftrightarrow u_{-1}^j = u_1^j, \\ \left. \frac{\partial u}{\partial x} \right|_{x=b} = 0 &\Leftrightarrow \frac{u_{M+1}^j - u_{M-1}^j}{2\Delta x} = 0 \Leftrightarrow u_{M+1}^j = u_{M-1}^j. \end{aligned}$$

One can try to rewrite the differential scheme to more general matrix form. In matrix notation the second time-row is given by

$$\boxed{\mathbf{u}^1 = \Delta t \boldsymbol{\gamma}_1 + A \mathbf{u}^0 - \frac{\Delta t^2}{2} \boldsymbol{\beta}_1}, \quad (5.11)$$

where

$$\boldsymbol{\gamma}_1 = (g(a), g(x_1), g(x_2), \dots, g(x_{M-1}), g(b))^T \quad \text{and}$$

$$\boldsymbol{\beta}_1 = (\sin(u_0^0), \sin(u_1^0), \dots, \sin(u_{M-1}^0), \sin(u_M^0))^T$$

are $M + 1$ -dimensional vectors and A is a tridiagonal square $M + 1 \times M + 1$ matrix of the form

$$A = \begin{pmatrix} 1 - \alpha^2 & \boxed{\alpha^2} & 0 & \dots & 0 \\ \alpha^2/2 & 1 - \alpha^2 & \alpha^2/2 & \dots & 0 \\ 0 & \alpha^2/2 & 1 - \alpha^2 & \dots & 0 \\ \dots & \dots & \dots & \dots & \dots \\ 0 & \dots & \boxed{\alpha^2} & 1 - \alpha^2 & \dots \end{pmatrix}$$

The boxed elements indicate the influence of boundary conditions. Other time rows can also be written in the matrix form as

$$\boxed{\mathbf{u}^{j+1} = -\mathbf{u}^{j-1} + B \mathbf{u}^j - \Delta t^2 \boldsymbol{\beta}^j}, \quad j = 1, \dots, T - 1 \quad (5.12)$$

Here

$$\boldsymbol{\beta}^j = (\sin(u_0^j), \sin(u_1^j), \dots, \sin(u_{M-1}^j), \sin(u_M^j))^T$$

is a $M + 1$ -dimensional vector and B is a square matrix, defined by an equation

$$B = 2A.$$

Now we can apply the explicit scheme (5.9) described above to Eq. (5.1). Let us solve it on the interval $[-L, L]$ with no-flux boundary conditions using the following parameters set:

Space interval	$L=20$
Space discretization step	$\Delta x = 0.1$
Time discretization step	$\Delta t = 0.05$
Amount of time steps	$T = 1800$
Velocity of the kink	$c = 0.2$

We start with the numerical representation of kink and antikink solutions. The initial condition for the kink is

$$f(x) = 4 \arctan\left(\exp\left(\frac{x}{\sqrt{1-c^2}}\right)\right),$$

$$g(x) = -2 \frac{c}{\sqrt{1-c^2}} \operatorname{sech}\left(\frac{x}{\sqrt{1-c^2}}\right).$$

Figure 5.4 (a) shows the space-time plot of the numerical kink solution. For the antikink the initial condition reads

$$f(x) = 4 \arctan\left(\exp\left(-\frac{x}{\sqrt{1-c^2}}\right)\right),$$

$$g(x) = -2 \frac{c}{\sqrt{1-c^2}} \operatorname{sech}\left(\frac{x}{\sqrt{1-c^2}}\right).$$

Numerical solutions is shown on Fig. 5.4 (b).

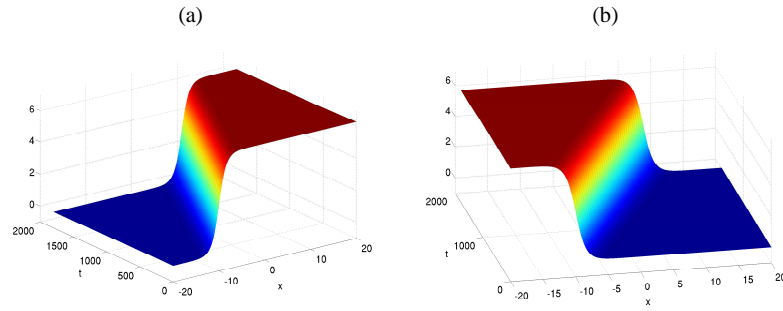


Fig. 5.4 Numerical solution of Eq. (5.1), calculated with the scheme (5.9) for the case of (a) the kink and (b) antikink solitons, moving with the velocity $c = 0.2$. Space-time information is shown.

Now we are in position to find numerical solutions, corresponding to kink-kink and kink-antikink collisions. For the kink-kink collision we choose

$$f(x) = 4 \arctan\left(\exp\left(\frac{x+L/2}{\sqrt{1-c^2}}\right)\right) + 4 \arctan\left(\exp\left(\frac{x-L/2}{\sqrt{1-c^2}}\right)\right),$$

$$g(x) = -2 \frac{c}{\sqrt{1-c^2}} \operatorname{sech}\left(\frac{x+L/2}{\sqrt{1-c^2}}\right) + 2 \frac{c}{\sqrt{1-c^2}} \operatorname{sech}\left(\frac{x-L/2}{\sqrt{1-c^2}}\right),$$

whereas for the kink-antikink collision the initial conditions are

$$f(x) = 4 \arctan\left(\exp\left(\frac{x+L/2}{\sqrt{1-c^2}}\right)\right) + 4 \arctan\left(\exp\left(-\frac{x-L/2}{\sqrt{1-c^2}}\right)\right),$$

$$g(x) = -2 \frac{c}{\sqrt{1-c^2}} \operatorname{sech}\left(\frac{x+L/2}{\sqrt{1-c^2}}\right) - 2 \frac{c}{\sqrt{1-c^2}} \operatorname{sech}\left(\frac{x-L/2}{\sqrt{1-c^2}}\right).$$

Numerical solutions, corresponding to both cases is presented on Fig. 5.5 (a)-(b), respectively. Finally, for the case of breather we choose

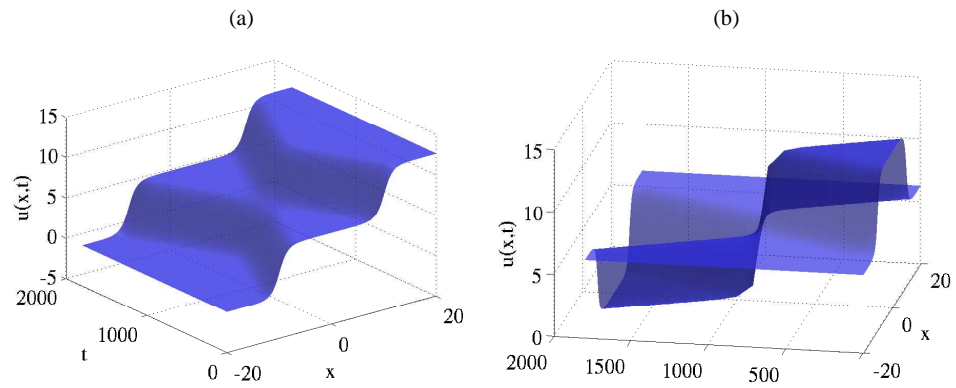


Fig. 5.5 Space-time representation of the numerical solution of Eq. (5.1) for (a) kink-kink collision and (b) kink-antikink collision.

$$f(x) = 0,$$

$$g(x) = 4\sqrt{1-c^2}\operatorname{sech}\left(x\sqrt{1-c^2}\right).$$

Corresponding numerical solution is presented on Fig. 5.6.

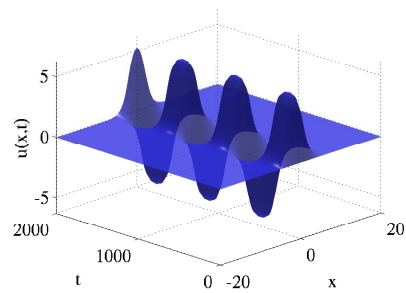


Fig. 5.6 Space-time plot of the numerical breather solution, oscillating with the frequency $\omega = 0.2$.

Appendix A

Tridiagonal matrix algorithm

The tridiagonal matrix algorithm (TDMA), also known as *Thomas algorithm*, is a simplified form of Gaussian elimination that can be used to solve tridiagonal system of equations

$$a_i x_{i-1} + b_i x_i + c_i x_{i+1} = y_i, \quad i = 1, \dots, n, \quad (\text{A.1})$$

or, in matrix form ($a_1 = 0, c_n = 0$)

$$\begin{pmatrix} b_1 & c_1 & 0 & \dots & \dots & 0 \\ a_2 & b_2 & c_2 & \dots & \dots & 0 \\ 0 & a_3 & b_3 & c_3 & \dots & 0 \\ \dots & \dots & \dots & \dots & c_{n-1} & \dots \\ 0 & \dots & \dots & 0 & a_n & b_n \end{pmatrix} \begin{pmatrix} x_1 \\ x_2 \\ \cdot \\ \cdot \\ x_n \end{pmatrix} = \begin{pmatrix} y_1 \\ y_2 \\ \cdot \\ \cdot \\ y_n \end{pmatrix}$$

The TDMA is based on the Gaussian elimination procedure and consist of two parts: a forward elimination phase and a backward substitution phase [15]. Let us consider the system (A.1) for $i = 1 \dots n$ and consider following modification of first two equations:

$$\text{Eq}_{i=2} \cdot b_1 - \text{Eq}_{i=1} \cdot a_2$$

which results in

$$(b_1 b_2 - c_1 a_2) x_2 + c_2 b_1 x_3 = b_1 y_2 - a_2 y_1.$$

The effect is that x_1 has been eliminated from the second equation. In the same manner one can eliminate x_2 , using the modified second equation and the third one (for $i = 3$):

$$(b_1 b_2 - c_1 a_2) \text{Eq}_{i=3} - a_3 (\text{mod. Eq}_{i=2}),$$

which would give

$$(b_3(b_1 b_2 - c_1 a_2) - c_2 b_1 a_3) x_3 + c_3(b_1 b_2 - c_1 a_2) x_4 = y_3(b_1 b_2 - c_1 a_2) - (y_2 b_1 - y_1 a_2) a_3$$

If the procedure is repeated until the n 'th equation, the last equation will involve the unknown function x_n only. This function can be then used to solve the modified equation for $i = n - 1$ and so on, until all unknown x_i are found (backward

substitution phase). That is, we are looking for a backward ansatz of the form:

$$x_{i-1} = \gamma_i x_i + \beta_i. \quad (\text{A.2})$$

If we put the last ansatz in Eq. (A.1) and solve the resulting equation with respect to x_i , the following relation can be obtained:

$$x_i = \frac{-c_i}{a_i \gamma_i + b_i} x_{i+1} + \frac{y_i - a_i \beta_i}{a_i \gamma_i + b_i} \quad (\text{A.3})$$

This relation possesses the same form as Eq. (A.2) if we identify

$$\boxed{\gamma_{i+1} = \frac{-c_i}{a_i \gamma_i + b_i}, \quad \beta_{i+1} = \frac{y_i - a_i \beta_i}{a_i \gamma_i + b_i}}. \quad (\text{A.4})$$

Equation (A.4) involves the recursion formula for the coefficients γ_i and β_i for $i = 2, \dots, n-1$. The missing values γ_1 and β_1 can be derived from the first ($i = 1$) equation (A.1):

$$x_1 = \frac{y_1}{b_1} - \frac{c_1}{b_1} x_2 \Rightarrow \gamma_2 = -\frac{c_1}{b_1}, \beta_2 = \frac{1}{b_1} \Rightarrow \boxed{\gamma_1 = \beta_1 = 0}.$$

The last what we need is the value of the function x_n for the first backward substitution. We can obtain it if we put the ansatz

$$x_{n-1} = \gamma x_n + \beta_n$$

into the last ($i = n$) equation (A.1):

$$a_n(\gamma x_n + \beta_n) + b_n x_n = y_n,$$

yielding

$$x_n = \frac{y_n - a_n \beta_n}{a_n \gamma_n + b_n}.$$

One can get this value directly from Eq. (A.2), if one formally puts

$$x_{n+1} = 0.$$

Altogether, the TDMA can be written as:

<p>1. Set $\gamma_1 = \beta_1 = 0$;</p> <p>2. Evaluate for $i = 1, \dots, n-1$</p> $\gamma_{i+1} = \frac{-c_i}{a_i \gamma_i + b_i}, \quad \beta_{i+1} = \frac{y_i - a_i \beta_i}{a_i \gamma_i + b_i};$ <p>3. Set $x_{n+1} = 0$;</p> <p>4. Find for $i = n+1, \dots, 2$</p> $x_{i-1} = \gamma_i x_i + \beta_i.$
--

The algorithm admits $\mathcal{O}(n)$ operations instead of $\mathcal{O}(n^3)$ required by Gaussian elimination.

Limitation

The TDMA is only applicable to matrices that are diagonally dominant, i.e.,

$$|b_i| > |a_i| + |c_i|, \quad i = 1, \dots, n.$$

Appendix B

The Method of Characteristics

The method of characteristics is a method which can be used to solve *an initial value problem* for general first order PDEs [4]. Let us consider a quasilinear equation of the form

$$A \frac{\partial u}{\partial x} + B \frac{\partial u}{\partial t} + Cu = 0, \quad u(x,0) = u_0, \quad (\text{B.1})$$

where $u = u(x,t)$, and A , B and C can be functions of independent variables and u . The idea of the method is to change coordinates from (x,t) to a new coordinate system (x_0,s) , in which Eq. (B.1) becomes *an ordinary differential equation* along certain curves in the (x,t) plane. Such curves, $(x(s),t(s))$ along which the solution of (B.1) reduces to an ODE, are called the *characteristic curves*. The variable s can be varied, whereas x_0 changes along the line $t = 0$ on the plane (x,t) and remains constant along the characteristics. Now if we choose

$$\frac{dx}{ds} = A, \quad \text{and} \quad \frac{dt}{ds} = B, \quad (\text{B.2})$$

then we have

$$\frac{du}{ds} = u_x \frac{dx}{ds} + u_t \frac{dt}{ds} = Au_x + Bu_t,$$

and Eq. (B.1) becomes the ordinary differential equation

$$\frac{du}{ds} + Cu = 0 \quad (\text{B.3})$$

Equations (B.2) and (B.3) give the characteristics of (B.1).

That is, a general strategy to find out the characteristics of the system like (B.1) is as follows:

- Solve Eq. (B.2) with initial conditions $x(0) = x_0$, $t(0) = 0$. Solutions of (B.2) give the transformation $(x,t) \rightarrow (x_0,s)$;
- Solve Eq. (B.3) with initial condition $u(0) = u_0(x_0)$ (where x_0 are the initial points on the characteristic curves along the $t = 0$ axis). So, we have a solution $u(x_0,s)$;

- Using the results of the first step find s and x_0 in terms of x and t and substitute these values in $u(x_0, s)$ to get the solution $u(x, t)$ of the original equation (B.1).

References

1. J. M. Burgers. *The Nonlinear Diffusion Equation*. D. Reidel, Dordrecht, 1974.
2. J. G. Charney, R. Fjoertoft, and J. von Neumann. Numerical integration of the barotropic vorticity equation. *Tellus*, 2:237–254, 1950.
3. J. D. Cole. On a quasi-linear parabolic equation occurring in aerodynamics. *Quarterly of Applied Mathematics*, 9:225–236, 1951.
4. R. Courant and D. Hilbert. *Methods of Mathematical Physics II*. Wiley, 1962.
5. R. Courant, E. Isaacson, and M. Rees. On the solution of non-linear hyperbolic differential equations. *Communications on Pure and Applied Mathematics*, 5:243–255, 1952.
6. J. Crank and P. Nicolson. A practical method for numerical evaluation of solutions of partial differential equations of the heat-conduction type. *Proceedings of the Cambridge Philosophical Society*, 43:50–67, 1947.
7. A. S. Davydov. *Solitons in Molecular Systems (Mathematics and its Applications)*. Dordrecht, Netherlands: Reidel, 1985, 1985.
8. S. Eule and R. Friedrich. A note on the forced burgers equation. *Physics Letters A*, 351:238, 2006.
9. E. Hopf. The partial differential equation $u_t + uu_x = u_{xx}$. *Communications on Pure and Applied Mathematics*, 3:201–230, 1950.
10. E. Isaacson and H. B. Keller. *Analysis of numerical Method*. Wiley, 1965.
11. G. L. Jr. Lamb. *Elements of Soliton Theory*. New York: Wiley, 1980.
12. P. D. Lax and B. Wendroff. Systems of conservation laws. *Communications on Pure and Applied Mathematics*, 13:217–237, 1960.
13. John H. Mathews and Kurtis D. Fink. *Numerical Methods Using Matlab*. Prentice Hall, New York, 1999.
14. A. M. Polyakov. Turbulence without pressure. *Physical Review E*, 52:6183–6188, 1995.
15. William H. Press, Saul A. Teukolsky, and William T. Vetterling. *Numerical Recipes in C: The Art of Scientific Computing*. Cambridge University Press, www.nr.com, 1993.
16. K. Friedrichs R. Courant and H. Lewy. Ueber die partiellen differenzengleichungen der mathematischen physik. *Mathematische Annalen*, 100(1):32–74, 1928.
17. M. Remoissenet. *Waves Called Solitons. Concepts and Experiments*. Springer, Berlin, 2003.
18. A. C. Scott. A nonlinear klein-gordon equation. *American Journal of Physics*, 37:52–61, 1969.
19. G. D. Smith. *Numerical Solution of Partial Differential Equations: Finite Difference Methods*. Oxford University Press, 3rd edition, 1985.
20. Josef Stoer and Roland Bulirsch. *Numerische Mathematik 2*. Springer, Berlin, 2000.
21. Michael Tabor. *Chaos and Integrability in Nonlinear Dynamics: An Introduction*. A Wiley-Interscience Publication, 1989.